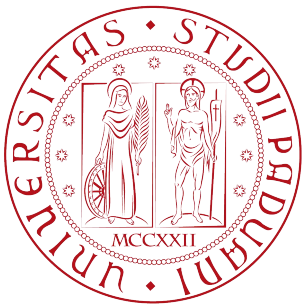

UNIVERSITÀ DEGLI STUDI DI PADOVA

Dipartimento di Fisica e Astronomia "Galileo Galilei"

Master Degree in Physics

Final Dissertation

The effect of the source on the Stochastic Gravitational Wave Background anisotropies

Thesis supervisor

Prof. Sabino Matarrese

Thesis co-supervisor

Dr. Angelo Ricciardone

Candidate

Alina Mierna

Academic Year 2021/2022

Contents

Introduction

The first direct detection of gravitational waves (GWs) was made in 2015 by the LIGO/Virgo collaboration [1]. It has also proven the existence of binary stellar-mass black hole systems. In 2017 the Advanced LIGO/Virgo collaboration made the first observation of a binary neutron star system [2]. In the future, many astrophysical sources are expected to be detected by aLIGO/Virgo and other planned detectors. However, the GWs are expected to discover not only new astrophysical objects but also to probe fundamental physics and cosmology. The GWs decouple from the rest of the components of the universe upon the production, therefore they can probe the energy scales inaccessible in any other way. However, to probe the physics of the early universe, the GW amplitude must be sufficiently large to be detected by current and future GW detectors. Several mechanisms in the early universe can generate a GW signal within the reach of GW detectors. The currently operating GW detectors include ground-based detectors, aLIGO, aVirgo, and KAGRA. The number of future GW detectors involves the ground-based interferometer Einstein Telescope (ET) [3], which is expected to be completed soon. The European Space Agency (ESA) has accepted the Laser Interferometer Space Antenna (LISA) [4], which will be the first space-based interferometer. The sensitivity of the Pulsar Timing Arrays to detect GWs is expected to improve in the future with the Square Kilometre Array [5]. There are also two other space-based projects, like DECIGO (DECi-hertz Interferometer Gravitational Wave Observatory) [6] and BBO (Big Bang Observer) [7].

The current ground-based interferometers are close to reaching the sensitivity necessary to detect the astrophysical GWB produced by a superposition of the signals from unresolved sources [8]. Future space-based and earth-based interferometers might be able to detect the cosmological GWB generated by inflation [9], preheating, phase transitions [10] or topological defects [11]. So we will require a method to differentiate the cosmological GW signal from the astrophysical one. The frequency dependence is one of the possible ways to distinguish among the various GW backgrounds since certain cosmological sources of GWs peak at some characteristic scales [12]. Although, due to the fact that future interferometers will have a much better angular resolution, angular anisotropies in the GW energy density could be an effective tool to distinguish among various sources of GWs in the early universe [13, 14, 15, 16]. The aim of this master thesis is to analyze the effect of different cosmological sources on the initial angular anisotropy of the SGWB.

In this thesis, we considered several mechanisms for the GW production in the early universe. The SGWB is expected from the amplification of initial quantum fluctuations of the tensor perturbations of the metric during inflation. However, inflation is not the only source of GWs expected in the early universe. In models beyond the standard single-field, additional fields may be present or new symmetries can be considered during inflation, which could also be the source of GWs. In the axion inflation model, the inflaton field is coupled to a gauge field, therefore besides the GWs from the vacuum fluctuations, we have the sourced GWs from the excited gauge field [17]. Another possibility is the presence of a second scalar field during inflation, the spectator field, which can induce GWs. Alternative to the standard inflationary model is the curvaton scenario, where the curvature perturbations are produced from an initial isocurvature perturbation associated with the quantum fluctuations of a curvaton field [18]. The SGWB is also expected to arise from strong first-order phase transitions. During a first-order phase transition, true vacuum bubbles nucleate and collide with each other in the background space-time, which is still in a false vacuum. Collisions of bubble walls break the spherical symmetry creating non-zero anisotropic stress and leading to the generation of GWs. Moreover, the expansion and collision of bubbles will induce sound waves and magneto-hydrodynamic turbulence, which also leads to the GW production. The relative contribution of these processes to the total GW spectrum depends on a specific particle physics model [10]. Furthermore, topological defects may arise as a result of symmetry-breaking phase transitions. Cosmic strings are one-dimensional topological defects produced as a result of a symmetry-breaking phase transition in the early universe. Cosmic strings may arise at the end of inflation in supersymmetric GUT models of Hybrid inflation [19]. Cosmic strings can also be the fundamental superstrings produced at the end of brane inflation [20]. Cosmic strings cross each other and reconnect forming smaller cosmic string loops. These loops begin to oscillate and decay emitting GWs [21].

To study the anisotropies of the SGWB, similarly to CMB anisotropies, we solve the Boltzmann equation for the graviton distribution function at first order around a FLRW metric [22, 23, 24]. The graviton distribution function can be expanded as a leading isotropic term plus a first-order anisotropic contribution. The isotropic and homogeneous part of the distribution function depends only on time and the GW frequency $p/2\pi$, where $\vec{p}$ is the physical momentum of the gravitons. In contrast to photons, the initial distribution of gravitons is not thermal leaving in the distribution the memory of the initial state. Due to the fact that the spectrum is not thermal, the angular anisotropies of the SGWB have an order one dependence on the GW frequency [25], while for the CMB anisotropies the dependence appears only at the second order. Furthermore, the CMB temperature anisotropies are generated only at the last scattering surface and thereafter, while GWs propagate freely at all energies below the Planck scale providing unique information about the physics of the early universe. Anisotropies in GW energy density are produced both at production and during their propagation through the large-scale scalar and tensor perturbations of the universe.

To fully describe the SGWB anisotropy we need to know the initial conditions for the GW energy density perturbation δ_{GW} and the evolution of gravitational potentials Φ and

Ψ. To this end, we solve the Einstein equations combined with the Boltzmann equation for various particle species present in the universe at the time of the GW production [26].

The primordial density perturbations can be split into adiabatic and isocurvature perturbations. Adiabatic perturbations are characterized by a vanishing entropy perturbation. Isocurvature perturbations have a non-vanishing entropy perturbation. The single-field models of inflation typically generate purely adiabatic perturbations. Isocurvature perturbations can be generated if more than one scalar field is present during inflation, for example, in inflationary models with the curvaton or spectator fields. Cosmic strings produce mainly isocurvature perturbations [27]. On the other hand, phase transitions can produce both adiabatic and isocurvature modes, depending on the given particle physics model [28]. In the case of adiabatic perturbations, GW energy density perturbations behave similarly to CMB anisotropies, even if there are some differences due to their non-thermal initial distribution. This is not necessarily the case for isocurvature perturbations. This can have an impact on the angular spectrum of the SGWB and can be a way to distinguish different sources of GW in the early Universe, being at the same time probes of the large-scale gravitational potentials.

We compute analytically the angular power spectrum of the SGWB. Then we implement numerically adiabatic and isocurvature initial conditions in the Boltzmann code CLASS, adapted for the SGWB [29].

The thesis is organized as follows. In Chapter 1 we give an overview of cosmological sources of GWs, which include inflation, phase transitions, and cosmic strings. In Chapter 2 we present the solution of the Boltzmann equation for GWs. Further, we decompose the solution of the Boltzmann equation in spherical harmonics and compute the angular power spectrum of the SGWB perturbations. In Chapter 3 we introduce the initial conditions for the GW energy density perturbation in the case of adiabatic and isocurvature perturbations. In Chapter 4 we provide the results of numerical computations in the Boltzmann code CLASS for the angular power spectrum of the initial condition term implementing different SGWB sources.

Chapter 1

Cosmological Sources of Gravitational Waves

1.1 Inflation

1.1.1 Quantum Fluctuations of the Inflaton Field

Inflation is a period of accelerated expansion in the early universe, which presents the solution to the shortcomings of the Hot Big Bang model such as the horizon and flatness problems [30]. Quantum fluctuations of the inflaton field stretch to the cosmological scales resulting in amplified classical density perturbations [31, 32, 33]. When the perturbations reenter the horizon they set the initial conditions for the Large Scale Structure formation. The simplest models of inflation predict adiabatic, Gaussian, and nearly scale-invariant density perturbations in a homogeneous and isotropic spatially flat universe. The intrinsic quantum fluctuations of the metric during inflation can generate GWs. The detection of GWs from inflation will allow us to probe the dynamics of inflation and allow us to differentiate among the specific models of inflation. The simplest models of inflation include an inflaton scalar field ϕ with a canonical kinetic term and potential $V(\phi)$, minimally coupled to gravity. The action for the inflaton scalar field reads [34]

$$S = \int d^4x\sqrt{-g}\left[\frac{m_{Pl}^2}{2}R - \frac{1}{2}\partial_\mu\phi\partial^\mu\phi + V(\phi)\right], \tag{1.1}$$

where R is the Ricci scalar and $m_{Pl} = 1/\sqrt{8\pi G}$ is a reduced Plank mass. To describe the evolution of a scalar field we can associate the stress-energy momentum to ϕ

$$T_{\mu\nu} = \frac{-2}{\sqrt{-g}}\frac{\delta S}{\delta g^{\mu\nu}} = \partial_\mu\phi\partial_\nu\phi + g_{\mu\nu}\left[\frac{1}{2}g^{\alpha\beta}\partial_\alpha\phi\partial_\beta\phi - V(\phi)\right]. \tag{1.2}$$

The inflaton field can be expressed as the sum of the classical background value, which is homogeneous and isotropic, and the quantum fluctuations

$$\begin{aligned}\phi\left(\vec{x},t\right)&=\langle 0|\phi\left(\vec{x},t\right)|0\rangle+\delta\phi\left(\vec{x},t\right)=\\&=\phi_0\left(t\right)+\delta\phi\left(\vec{x},t\right).\end{aligned}\tag{1.3}$$

The stress-energy momentum tensor for the classical background value is given by

$$T_0^0=-\left[\frac{1}{2}\dot{\phi}^2-V\left(\phi\right)\right]=-\rho_\phi,\tag{1.4}$$

$$T_j^i=\left[\frac{1}{2}\dot{\phi}^2-V\left(\phi\right)\right]\delta_j^i=\delta_j^iP_\phi.\tag{1.5}$$

The equation of state for the classical background value thus can be written as

$$w_\phi=\frac{P_\phi\left(t\right)}{\rho_\phi\left(t\right)}=\frac{\frac{1}{2}\dot{\phi}^2-V\left(\phi\right)}{\frac{1}{2}\dot{\phi}^2+V\left(\phi\right)}.\tag{1.6}$$

For inflation to occur it is required to have a negative isotropic pressure $P_\phi<0$. It is possible if $\frac{1}{2}\dot{\phi}^2\ll V\left(\phi\right)$, which brings to $P_\phi\approx-V(\phi)\approx-\rho_\phi$. The equation of state is $w_\phi\simeq-1$, giving rise to a quasi-de-Sitter phase with a quasi-exponential expansion $a(t)\approx e^{Ht}$, where a Hubble rate H approximately constant. This condition is realized if we consider a sufficiently flat potential $V\left(\phi\right)\approx const$, which is called a slow-roll regime. The equation of motion for the scalar field from the variational principle is

$$\frac{\delta S}{\delta\phi}=0.\tag{1.7}$$

In the spatially flat FRW metric it takes the form

$$\ddot{\phi}+3H\dot{\phi}-\frac{\nabla^2\phi}{a^2}=-\frac{\partial V}{\partial\phi}.\tag{1.8}$$

For the classical background value of the scalar field, the equation reads

$$\ddot{\phi}+3H\dot{\phi}=-\frac{\partial V}{\partial\phi}.\tag{1.9}$$

Two conditions must be fulfilled to realize inflation for a sufficiently long amount of time to solve the shortcomings of the Hot Big Bang model. The first slow roll condition is

$$\frac{1}{2}\dot{\phi}^2\ll V\left(\phi\right).\tag{1.10}$$

We introduce the second slow roll condition

$$\ddot{\phi}\ll3H\dot{\phi}.\tag{1.11}$$

It ensures that we have an asymptotic attractor solution to the equation of motion

$$\dot{\phi} \simeq -\frac{V'}{3H}. \tag{1.12}$$

In order to quantify the slow-roll regime dynamics, it is also useful to define the two slow-roll parameters

$$\begin{aligned} \epsilon &= -\frac{\dot{H}}{H} \simeq \frac{3}{2}\frac{\dot{\phi}^2}{V(\phi)}, \\ \eta &= -\frac{\ddot{\phi}}{H\dot{\phi}}, \end{aligned} \tag{1.13}$$

exploiting the slow roll conditions the parameters must satisfy $\epsilon \ll 1$ and $\eta \ll 1$. Although $\epsilon \ll 1$ is sufficient to have inflation, the condition $\eta \ll 1$ will ensure that inflation lasts for long enough.

As aforementioned the perturbations of the inflaton field will induce the tensor perturbations of the metric producing the SGWB. The perturbed spatially flat FLRW metric, neglecting scalar and vector perturbations, is [34]

$$ds^2 = a^2(\eta)\left[-d\eta^2 + (\delta_{ij} + h_{ij})\, dx^i dx^j\right], \tag{1.14}$$

with h_{ij} such that $h_{ij} = h_{ji}$,$h^i_i = 0$,$h^i_{j|i} = 0$. The equation of motion for h_{ij} is obtained from the Einstein equation

$$\frac{\delta S}{\delta g_{\mu\nu}} = 0, \tag{1.15}$$

around the metric in eq. (1.14), then we get

$$h''_{ij} + 2\mathcal{H}h'_{ij} - \frac{\nabla^2 h_{ij}}{a^2} = 16\pi G a^2 \Pi^{TT}_{ij}, \tag{1.16}$$

where $\mathcal{H}$ is the conformal Hubble rate and Π^{TT}_{ij} is a traceless and transverse component of an anisotropic stress tensor. The anisotropic stress is given by $a^2\Pi_{ij} = T_{ij} - pa^2(\delta_{ij} + h_{ij})$, where T_{ij} is the spatial components of the energy-momentum tensor of the source and p is the background pressure. It vanishes at first order for single field inflation, therefore

$$h''_{ij} + 2\mathcal{H}h'_{ij} - \frac{\nabla^2 h_{ij}}{a^2} = 0. \tag{1.17}$$

Since h_{ij} is symmetric, transverse, and trace-free, tensor perturbations have two physical degrees of freedom, so it can be decomposed in a Fourier space as

$$h_{ij} = \sum_{\lambda=+,\times} \int \frac{d^3k}{(2\pi)^3} e^{i\vec{k}\cdot\vec{x}} h_\lambda\left(\vec{k},\vec{\tau}\right) \epsilon^\lambda_{ij}\left(\vec{k}\right), \tag{1.18}$$

where $\epsilon^\lambda_{ij}\left(\vec{k}\right)$ is the polarization tensor, which satisfies $\epsilon_{ij} = \epsilon_{ji}$, $\epsilon^i_i = 0$, $k^i\epsilon_{ij} = 0$, and the normalization condition $\epsilon^\lambda_{ij}\epsilon^{ij}_{\lambda'} = \delta_{\lambda\lambda'}$. The equation of motion becomes

$$h_\lambda'' + 2\mathcal{H}h_\lambda' - \frac{k^2 h_\lambda}{a^2} = 0, \tag{1.19}$$

which is analogous to the equation of motion for a minimally coupled scalar field. We can parametrize it as

$$h_\lambda = \frac{\sqrt{2}}{m_{Pl}} \frac{v_\lambda\left(\eta, \vec{k}\right)}{a}. \tag{1.20}$$

Since we are considering the quantum fluctuations, we have to quantize the inflaton field. We apply the canonical quantization for $v_\lambda\left(\eta, \vec{k}\right)$

$$v_\lambda\left(\eta, \vec{k}\right) = \int \frac{d^3k}{(2\pi)^3}\left[v_k(\eta)\, e^{-i\vec{k}\vec{x}} \hat{a}_{\vec{k},\lambda} + v_k(\eta)\, e^{-i\vec{k}\vec{x}} \hat{a}^+_{\vec{k},\lambda}\right], \tag{1.21}$$

where $a_{\vec{k},\lambda}, a^+_{\vec{k},\lambda}$ are the annihilation and creation operators respectively. The normalization condition for $v_\lambda\left(\eta, \vec{k}\right)$ is

$$v_k v_k^{*'} - v_k^* v_k' = i. \tag{1.22}$$

which ensures the canonical commutation relation for $\hat{a}_{\vec{k},\lambda}$ and $\hat{a}^+_{\vec{k},\lambda}$

$$\begin{aligned} \left[\hat{a}_{\vec{k},\lambda}, \hat{a}^+_{\vec{k}',\lambda'}\right] &= (2\pi)^3 \delta_{\lambda\lambda'} \delta^{(3)}\left(\vec{k} - \vec{k'}\right) \\ \left[\hat{a}^+_{\vec{k},\lambda}, \hat{a}^+_{\vec{k}',\lambda'}\right] &= \left[\hat{a}_{\vec{k},\lambda}, \hat{a}_{\vec{k}',\lambda'}\right] = 0. \end{aligned} \tag{1.23}$$

Hence, the equation of motion can be rewritten as

$$v_k''(\eta) + \left(k^2 - \frac{a''}{a}\right) v_k(\eta) = 0. \tag{1.24}$$

We can relate a conformal time and a Hubble rate at first order as

$$\eta \simeq \frac{1}{\mathcal{H}(1-\epsilon)}, \tag{1.25}$$

then the term involving the scale factor in eq. (1.24) is

$$\frac{a''}{a} = \mathcal{H}' + \mathcal{H}^2 \simeq (2-\epsilon)\mathcal{H}^2 \simeq \frac{1}{\eta^2}(2+3\epsilon), \tag{1.26}$$

and the equation of motion can be written as

$$v_k''(\eta) + \left(k^2 - \frac{v^2 - \frac{1}{4}}{\eta^2}\right) v_k(\eta) = 0, \tag{1.27}$$

where $\nu^2 = \frac{9}{4} + 3\epsilon$. This is a Bessel equation, whose solution is of the form

$$v_\lambda\left(\eta,\vec{k}\right)=\sqrt{-\eta}\left[c_1\left(k\right)H_\nu^{(1)}\left(-k\nu\right)+c_2\left(k\right)H_\nu^{(2)}\left(-k\nu\right)\right], \tag{1.28}$$

where $H_\nu^{(1)}\left(-k\nu\right)$ and $H_\nu^{(2)}\left(-k\nu\right)=H_\nu^{(1)*}\left(-k\nu\right)$ are the Hankel functions of the first and second kind. On sub-horizon scales, $-k\eta\gg 1$, we want to be able to reproduce a flat spacetime metric, thus we require a plane wave solution on sub-horizon scales

$$v_k\left(\eta\right)=c_{k,+}e^{-ik\eta}+c_{k,-}e^{ik\eta}. \tag{1.29}$$

We set $c_{k,-}=0$ as initial condition and the value of $c_{k,+}$ is determined by the normalization condition in eq. (1.22). The solution then is

$$v_k\left(\eta\right)=\frac{1}{\sqrt{2k}}e^{-ik\eta}, \tag{1.30}$$

and given that for $-k\eta\gg 1$

$$H_\nu^{(1)}\left(-k\nu\right)\simeq\sqrt{\frac{2}{\pi}}\frac{e^{-ik\nu}}{\sqrt{-k\nu}}\frac{1}{\sqrt{2k}}e^{-ik\eta}, \tag{1.31}$$

we must impose $c_2=0$ and $c_1=\frac{\sqrt{\pi}}{2}e^{i\left(v+\frac{1}{2}\right)\frac{\pi}{2}}$. The exact solution then becomes

$$v_k\left(\eta\right)=\frac{\sqrt{\pi}}{2}e^{i\left(v+\frac{1}{2}\right)\frac{\pi}{2}}\sqrt{-\eta}H_v^{(1)}\left(-k\eta\right), \tag{1.32}$$

and on superhorizon scales, $-k\eta\ll 1$, we have

$$H_\nu^{(1)}\left(-k\nu\right)\simeq\sqrt{\frac{2}{\pi}}e^{-i\frac{\pi}{2}}2^{v-\frac{3}{2}}\frac{\Gamma\left(\nu\right)}{\Gamma\left(\frac{3}{2}\right)}\left(-k\eta\right)^{-\nu}, \tag{1.33}$$

then the solution reduces to

$$v_k\left(\eta\right)=\frac{1}{\sqrt{2k}}e^{i\left(v-\frac{1}{2}\right)\frac{\pi}{2}}2^{v-\frac{3}{2}}\frac{\Gamma\left(\nu\right)}{\Gamma\left(\frac{3}{2}\right)}\left(-k\eta\right)^{\frac{1}{2}-\nu}. \tag{1.34}$$

Writing the original field as

$$h_{ij}=\sum_{\lambda=+\times}\int\frac{d^3k}{\left(2\pi\right)^3}\left[h_k\left(\eta\right)e^{-i\vec{k}\vec{x}}a_{\vec{k},\lambda}+h_k\left(\eta\right)e^{-i\vec{k}\vec{x}}a^+_{\vec{k},\lambda}\right]\epsilon_{ij}^\lambda\left(\vec{k}\right), \tag{1.35}$$

and using eq. (1.20) and eq. (1.34) we obtain the amplitude of the physical tensor modes h_{ij} at superhorizon scales

$$\left|h_\lambda\right|\simeq\frac{H}{m_{Pl}\sqrt{k^3}}\left(\frac{k}{aH}\right)^{-\epsilon}, \tag{1.36}$$

which at horizon crossing $k=a_kH_k$, reduces to

$$\left|h_\lambda\right|\simeq\frac{H_k}{m_{Pl}\sqrt{k^3}}, \tag{1.37}$$

We define a dimensionless tensor power spectrum $P_h(k)$ as

$$\langle h_{ij,\lambda}(\vec{k},\eta)h^*_{ij,\lambda}(\vec{k}',\eta)\rangle = \frac{2\pi^2}{k^3}\delta_{\lambda\lambda'}P_h(k)\delta^{(3)}(\vec{k}-\vec{k}'), \tag{1.38}$$

using eq. (1.35) and eq. (1.23) we find

$$\left\langle h_{ij}\left(\vec{k},\eta\right)h^*_{ij}\left(\vec{k},\eta\right)\right\rangle = 2\delta^{(3)}\left(\vec{k}-\vec{k}'\right)|h_k(\eta)|^2. \tag{1.39}$$

Finally, we obtain the inflationary tensor power spectrum

$$P_h(k) = \frac{2}{\pi^2}\frac{H^2}{m_{Pl}^2}\left(\frac{k}{aH}\right)^{-2\epsilon}, \tag{1.40}$$

which at horizon crossing $k = a_k H_k$, reduces to

$$P_h(k) = \frac{2}{\pi^2}\frac{H_k^2}{m_{Pl}^2}, \tag{1.41}$$

We can define the spectral index for the tensor modes that describe the shape of the power spectrum as

$$n_T = \frac{d\ln P_h(k)}{d\ln k}, \tag{1.42}$$

applying eq. (1.40) we get

$$n_T \simeq -2\epsilon. \tag{1.43}$$

In the simplest models of inflation $\epsilon > 0$ and so n_T is expected to be red tilted, namely it decreases on smaller scales. The red tilt of the tensor power spectrum is a consequence of the fact that the amplitude at horizon crossing is directly proportional to the energy scale of inflation, $H_k^2 \approx V(\phi)/m_{Pl}^2$, since the Hubble rate decreases slowly during inflation.

After the tensor modes cross the horizon during inflation, they remain constant, therefore eq. (1.37) will provide the initial condition for the modes that reenter the horizon in a post-inflationary epoch. When the tensor modes reenter the horizon, they obtain a time dependence, starting to oscillate and decay as $1/a$. A general solution today can be written as [35]

$$h(k,\eta_0) = T(k,\eta_0)\, h_{inf}(k), \tag{1.44}$$

where $T(k,\eta_0)$ is the transfer function that describes the evolution of perturbations. It can be written as

$$T(k,\eta_0) = \begin{cases} \frac{3j_1(k\eta_0)}{k\eta_0} & k < k_{eq}, \\ \frac{A(k)}{h_{inf}(k)}\frac{j_1(k\eta_0)}{k\eta_0} + \frac{B(k)}{h_{inf}(k)}\frac{j_1(k\eta_0)}{k\eta_0} & k > k_{eq}, \end{cases} \tag{1.45}$$

where k_* is wave number and $A(k)$, $B(k)$ are the matching coefficients at radiation-matter equality. The GW energy density from inflation today is

$$\begin{aligned}\rho_{GW}(\eta_0) &= \frac{\langle h'_{ij}(\vec{x},\eta_0)\, h^{ij'}(\vec{x},\eta_0)\rangle}{32\pi G a_0^2} = \\ &= \frac{1}{64\pi^3 G a_0^2}\int dk k^2 \left[T'(k,\eta_0)\right]^2 |h_{inf}(k)|^2 .\end{aligned} \tag{1.46}$$

The spectral GW energy density from inflation today reads

$$\Omega_{\rm GW}(k) = \frac{1}{\rho_c}\frac{{\rm d}\rho_{GW}}{{\rm d}\ln k} = \frac{1}{12H_0^2 a_0^2}\left[T'(k,\eta_0)\right]^2 P_h(k), \tag{1.47}$$

where we used $\rho_c = 3H^2/8\pi G$. Typically, we are interested in the solution at sub-horizon scales, where the transfer function is given by

$$T'(k,\eta_0) = \begin{cases} \frac{\eta_{eq}^2}{2\eta_0^4} & k < k_{eq}, \\ \frac{9}{2\eta_0^4 k^2} & k > k_{eq}. \end{cases} \tag{1.48}$$

An upper bound from the CMB on the amplitude of SGWB generated during inflation is [34]

$$\Omega_{GW}^{CMB} = 5\times 10^{-16}\left(\frac{H_{inf}}{H_{max}}\right)^2, \tag{1.49}$$

where H_{inf} is the inflationary Hubble rate, evaluated at the CMB scales, $f_{CMB} \approx 10^{-18} - 10^{-17} Hz$, and H_{max} is the current upper bound on the energy scale of inflation, $H_{max} \approx 8.8\times 10^{13} GeV$ [36]. We can parametrize the GW spectrum by a power law relative to a pivot scale at the CMB frequencies [9],

$$\Omega_{GW} = \Omega_{GW}^{CMB}\left(\frac{f}{f_{CMB}}\right)^{n_T}. \tag{1.50}$$

For the standard single-field models of inflation, the consistency relation must be satisfied [37]

$$r = -8 n_T, \tag{1.51}$$

where $r = P_h/P_\phi$ is the tensor-to-scalar ratio, P_h and P_ϕ are the tensor and scalar power spectra respectively. In standard inflationary models $n_T < 0$ with $|n_T| \ll 1$ and from the current CMB bounds $r \leq 0.014$ [38].

Even in the case of an almost scale-invariant spectrum, the GW amplitude is below the sensitivity of current ground-based interferometers such as LIGO and Virgo. The sensitivity of aLIGO is $h^2 \approx 10^{-9}$ [39]. in the frequency range $10Hz \leq f \leq 10kHz$. The third generation ground-based future interferometer Einstein Telescope will allow to probe the stochastic background down to $\Omega_{GW}h^2 \approx 10^{-12}$ for the frequency range $1Hz \leq f \leq 10kHz$ [3]. Another planned experiment is LISA, which is a space-based

interferometer, therefore it can reach much lower frequencies in the range $10^{-5}Hz \leq f \leq 1Hz$. LISA is expected to probe a SGWB down to a level of $\Omega_{GW}h^2 \approx 10^{-13}$ [40]. If the energy scale of inflation is high enough, future GW detectors such as Big Bang Observatory (BBO) [41] and Deci-hertz Interferometer Gravitational wave Observatory (DECIGO) [42] might be able to detect the irreducible GW background from inflation. The approximate lower bound on the GW signal for BBO and DECIGO is $\Omega_{GW}h^2 \approx 10^{-16}$.

1.1.2 Axion Inflation

However, the quantum fluctuations of the metric maybe not be the only source of GWs during inflation. In models beyond the standard single field models, additional fields may be present or new symmetries are considered during inflation, which would change the GW spectrum significantly. The corresponding GW signal can overtake the irreducible GW background from vacuum fluctuations. Contrary to the GW from vacuum fluctuations, these models can generate a comparably large and blue-tilted GW spectrum providing an attractive target for future GW interferometers.

Let us consider the scenario, where the inflaton ϕ is a pseudo-scalar field and it is coupled with a gauge field A_μ, which is excited as the inflaton rolls down its potential [17]. The Lagrangian interaction term is of the form

$$\Delta L = -\frac{1}{4f}\phi F_{\mu\nu}\tilde{F}^{\mu\nu}, \tag{1.52}$$

where f is the decay constant of the inflaton field. The equation of motion for ± 1-helicity odes $A_\pm(\vec{k},\eta)$ of the gauge field is [43]

$$A''_\pm\left(\vec{k},\eta\right) + \left[k^2 \pm 2\xi\frac{k}{\eta}\right] A_\pm\left(\vec{k},\eta\right) = 0, \tag{1.53}$$

where ξ is the parameter that characterizes the strength of the inflaton-gauge coupling

$$\xi = \frac{\dot{\phi}}{2fH}. \tag{1.54}$$

For wavelengths $-k\eta > 2\xi$, one of the two helicity modes $A_\pm\left(\vec{k},\eta\right)$ is exponentially amplified during inflation. Hence, the excited gauge field is able to generate a strong GW signal. The fact that only one of the polarization modes is amplified is a reflection of the parity violation of the operator in eq. (1.52). The energy-momentum tensor of the gauge field is quadratic in the fields, therefore the tensor modes produced by the gauge field obey non-Gaussian statistics.

From the constraints on the non-Gaussianity at the CMB scales by the Planck experiment, $\xi < 2.5$ [44]. The GW signal for such values of ξ is below the sensitivity of the current and future experiments. However, the parameter ξ is a time-dependent quantity, which will increase on smaller scales, since $\dot{\phi}$ increases and H decreases near the end of

inflation. Thus it is possible to have the Planck constraints on the power spectra and non-Gaussianity at the CMB scales satisfied and simultaneously have a large GW signal at smaller scales.

The total tensor power spectrum consists of the sum of the power spectra of vacuum fluctuations and sourced GWs from the excited gauge field [45]

$$\begin{aligned} P_h^{total}(k) &= \frac{k^3}{2\pi^2}\sum_{\lambda=\pm}|h_\lambda(k)|^2 = P_h^{vac}(k) + P_h^{sourced}(k) \\ &= \frac{2H^2}{\pi^2 M_{Pl}^2} + 8.7\times 10^{-8}\frac{H^4}{M_{Pl}^4}\frac{e^{4\pi\xi}}{\xi^6}. \end{aligned} \tag{1.55}$$

From the power spectrum P_h we can readily get the spectral GW energy density $h^2\Omega_{\rm GW}$. Figure 1.1 depicts the spectral GW energy density as a function of the frequency for $f = m_{Pl}/35$ with a quadratic inflaton potential $V(\phi) = \frac{1}{2}m^2\phi^2$. At large scales $\left(f \leq 10^{-5}\text{Hz}\right)$ a leading contribution comes from the vacuum fluctuations. At intermediate scales, $\left(10^{-5}\,\text{Hz} \leq f \leq 1\,\text{Hz}\right)$ the sourced GWs dominate over the vacuum fluctuations, although the back reaction of the gauge field on the inflaton field is negligible. At small scales, $(f \geq 1Hz)$ the back reaction of the gauge field cannot be neglected anymore. The conservation of energy implies that the production of photons reduces the kinetic energy of the inflaton, therefore the growth of $\dot{\phi}$ is slowed down, resulting in a flattening of $h^2\Omega_{GW}$ at the smallest scales. Since $\dot{\phi}$ and H increase and decrease respectively over time, the power spectrum of the sourced GWs is typically blue tilted.

The spectral energy density of the sourced GWs reads

$$\Omega_{GW}h^2 = 1.5\times 10^{-13}\frac{H^4}{M_{Pl}^4}\frac{e^{4\pi\xi}}{\xi^6}, \tag{1.56}$$

where H and ξ are evaluated at the horizon crossing for a given mode. It can be locally parameterized as $\Omega_{GW}h^2 \approx f^{n_T}$ at a given frequency f. At any frequency, we can define the spectral tilt as

$$n_T = \frac{d\ln\Omega_{GW}h^2}{d\ln f}, \tag{1.57}$$

and at first order in slow-roll parameters, it reads [9]

$$n_T \simeq -4\epsilon + (4\pi\xi - 6)(\epsilon - \eta). \tag{1.58}$$

For the range of ξ that future interferometers can probe ($\zeta \geq 3.5$ for LISA [9]), the term -4ϵ is negligible in comparison with the other term, so the spectral tilt can be approximated as

$$n_T \simeq (4\pi\xi - 6)(\epsilon - \eta). \tag{1.59}$$

This simplification allows us to obtain a model-independent parameter estimation related to the sensitivity of a given GW detector.

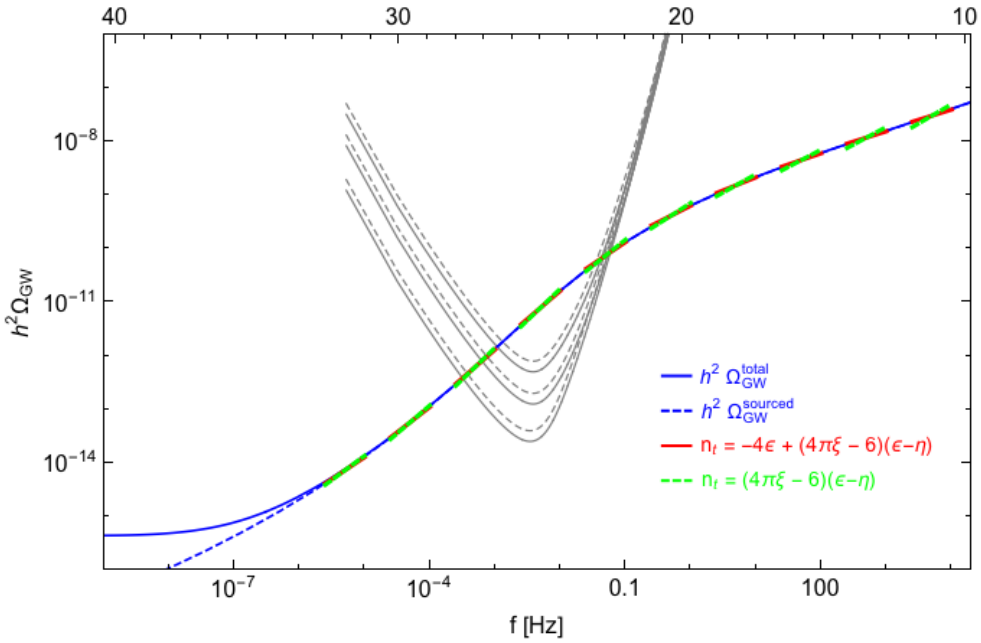

Figure 1.1: GW spectrum today $h^2\Omega_{GW}$ from a numerical integration versus the local parameterization $\Omega_{GW}h^2 \approx (f/f_*)^{n_T}$ evaluated at different pivot frequencies f_* with the spectral tilt n_T obtained from successive approximations [9].

To summarize, the amplification mechanism from the gauge field gives rise to the significant blue tilted GW signal that can be probed by the upcoming experiments. The parity violation and highly non-Gaussian statistics are also distinctive features of this mechanism [9].

1.1.3 Inflation with spectator field

Isocurvature perturbations can be generated if more than one scalar field is present during inflation. However, the presence of isocurvature perturbations does not necessarily lead to the GW production. The other scalar fields, besides the inflaton, which are present during inflation, are referred to as spectator fields. The presence of a spectator field gives rise to a second-order source term in the equation of motion of GWs leading to a classical production of GWs. Let us consider a Lagrangian of the form [46]

$$L = \frac{1}{2}m_{Pl}^2 R + \frac{1}{2}\partial_\mu\phi\partial^\mu\phi - V(\phi) + P(X,\sigma), \tag{1.60}$$

where ϕ is the inflaton field and σ is the spectator field, $X = \frac{1}{2}\partial_\mu\sigma\partial^\mu\sigma$ and P is a generic function of X and σ. The inflaton field drives the cosmological expansion and also generates the scalar perturbations. The spectator field does not play a role in

the dynamics of inflation, but it still can produce scalar and tensor perturbations. The propagation speed of the spectator field perturbations is

$$c_s = \frac{P_X}{P_X + P_{XX}\dot{\sigma}_0^2}, \tag{1.61}$$

where σ_0 is the background value. We consider the models with $c_s \ll 1$, since it leads to a more efficient GW production compared to $c_s = 1$. The value of c_s can change during inflation and this variation is characterized by a parameter

$$s = \frac{\dot{c}_s}{Hc_s} \neq 0, \tag{1.62}$$

which is assumed to be a small quantity. The total power spectrum of the GWs from inflation consists of the irreducible GW background from vacuum fluctuations of the metric and the classical GW production by the spectator field. Both of these contributions can be characterized by a power law. Likewise, the scalar perturbations are generated by the vacuum perturbations and the spectator field, also following a power law. We can then write the total tensor and scalar power spectra, respectively, as

$$P_{\mathrm{GW}}(k) = A_T^{(v)}(k_*)\left(\frac{k}{k_*}\right)^{n_T^{(v)}} + A_T^{(\sigma)}(k_*)\left(\frac{k}{k_*}\right)^{n_T^{(\sigma)}}, \tag{1.63}$$

and

$$P_S(k) = A_S^{(v)}(k_*)\left(\frac{k}{k_*}\right)^{n_S^{(v)}-1} + A_S^{(\sigma)}(k_*)\left(\frac{k}{k_*}\right)^{n_S^{(\sigma)}-1}, \tag{1.64}$$

where k_* is the pivot scale. The scalar and tensor power spectra can be obtained by perturbing the action at third order. This leads to a term $h_{ij}\delta\sigma\delta\sigma$, which gives rise to the sourced GWs. The equation of motion for tensor perturbations is given by

$$h_{ij}'' + 2\mathcal{H}h_{ij} - \partial_k^2 h_{ij} = \frac{2P_X}{m_{Pl}^2}\left[\partial_i\delta\sigma\partial_j\delta\sigma\right]^{TT}. \tag{1.65}$$

The amplitude of tensor perturbations then at a given pivot scale can be approximated as

$$A_T^{(\sigma)} \simeq \frac{8}{15\pi c_S^3}\frac{H^4}{m_{Pl}^4}, \tag{1.66}$$

where H and c_s are evaluated at the pivot scale. Furthermore, the amplitude of the sourced scalar contribution at the pivot scale is

$$A_S^{(\sigma)} \simeq \frac{1}{32\pi c_S^7}\frac{H^4}{m_{Pl}^4}, \tag{1.67}$$

where H and c_s are evaluated at the pivot scale. We can obtain the corresponding spectral indexes at the lowest order in the parameters ϵ and s

$$
\begin{aligned}
n_T^{(\sigma)} &= -4\epsilon - 3s, \\
n_S^{(\sigma)} - 1 &= -4\epsilon - 7s.
\end{aligned}
\tag{1.68}
$$

We focus on the cases, where $s \neq 0$ and $|s| < 0$, thereby the GW amplitude is enhanced on small scales. Finally, the total tensor and scalar power spectra, respectively, are

$$
P_{GW}(k) = \frac{2H^2}{m_{Pl}^2}\left(\frac{k}{k_*}\right)^{n_T^{(v)}} + \frac{8}{15\pi c_S^3}\frac{H^4}{m_{Pl}^4}\left(\frac{k}{k_*}\right)^{n_T^{(\sigma)}}, \tag{1.69}
$$

and

$$
P_S(k) = \frac{H^2}{4\epsilon m_{Pl}^2}\left(\frac{k}{k_*}\right)^{n_S^{(v)}-1} + \frac{1}{32\pi c_S^7}\frac{H^4}{m_{Pl}^4}\left(\frac{k}{k_*}\right)^{n_S^{(\sigma)}-1}. \tag{1.70}
$$

Both the scalar and tensor power spectra are determined by the energy scale of inflation through the Hubble rate H, the slow-roll parameters, and specific parameters c_s and s. If c_s is small enough and s is negative, but $|s| \gg 1$, the sourced GW spectrum is blue tilted. Thus, the sourced GWs could have a sufficiently large amplitude, detectable by LISA, while the amplitude is small at the CMB scales.

If the spectator field σ is stable and decays late enough after the end of inflation it is possible to have isocurvature perturbations.

1.1.4 Curvaton scenario

In the standard slow-roll single-field models of inflation, the observed density perturbations are generated by the fluctuations of the inflaton field. These models lead to adiabatic perturbations. Another possibility is the curvaton scenario, where the curvature perturbations are generated by an initial isocurvature perturbation related to the quantum fluctuations of another light scalar field. The curvaton energy density is negligible during inflation. When the curvaton decays into radiation after the end of inflation the isocurvature perturbations are converted into adiabatic ones.

In the curvaton scenario, the total curvature perturbation can evolve on large scales due to a non-adiabatic pressure perturbation [47, 48]. During inflation, isocurvature perturbations of the curvaton field σ are generated [18]

$$
\delta\sigma_k = \frac{H_*}{2\pi}. \tag{1.71}
$$

In the radiation-dominated epoch, after the inflation, the curvaton field oscillates, which leads to the change in the energy density and therefore transformation of the initial isocurvature perturbations into the curvature ones. The energy density perturbation of the curvaton field is given by

$$
\frac{\delta\rho_\sigma}{\sigma_\sigma} \simeq \frac{\delta\sigma_k}{\overline{\sigma}_*}, \tag{1.72}
$$

where $\overline{\sigma}_*$ is the value of the classical curvaton field during inflation. The curvature perturbation ζ is negligible when the curvaton begins to oscillate and is constant when the curvaton decays. If the curvaton decays instantaneously then the curvature perturbation is given by

$$\zeta_k \simeq r\frac{\delta\sigma_k}{\overline{\sigma}_*}, \tag{1.73}$$

where $r = (\rho_\sigma/\rho)_D$ is the fraction of the curvaton energy density to the total and D denotes the decay time. The corresponding power spectrum is

$$P_\zeta^{1/2} \simeq r\frac{H_*}{2\pi\overline{\sigma}_*}. \tag{1.74}$$

We have a nearly scale-invariant power spectrum if we assume that the curvaton field is effectively massless during inflation. The power spectrum of GWs from inflation is [34]

$$P_h \simeq \frac{2}{2m_{Pl}^2}\frac{H_*^2}{\pi^2}. \tag{1.75}$$

In the curvaton scenario, the initial curvature perturbation of the inflaton field is negligible. In the standard slow-roll models of inflation, the curvature perturbations are induced by the inflaton field and the power spectrum of the curvature perturbation is given by [18]

$$P_\zeta \simeq \frac{1}{2m_{Pl}^2\epsilon}\left(\frac{H_*}{2\pi}\right)^2\left(\frac{k}{aH_*}\right)^{n_\zeta-1}, \tag{1.76}$$

where $n_\zeta \simeq 1$ denotes the spectral index and ϵ is the standard slow-roll parameter given by

$$\epsilon = \frac{\dot{\phi}^2}{2m_{Pl}^2H_*^2}. \tag{1.77}$$

Furthermore, the GWs are produced at second order by the curvature perturbations. In the curvaton scenario, the GW production through the curvature perturbations takes place only when the curvaton decays, namely when the isocurvature perturbations transform into curvature fluctuations. The GWs produced by the curvaton perturbations between the end of inflation and the time of curvaton decay are isocurvature. The contribution from these perturbations is directly proportional to the amount of non-Gaussianity in the curvaton scenario [49]. The current constrain on the non-Gaussianity from Plank data is $|f_{NL}| \leq -0.9$ [50].

The equation of motion for the GWs in Fourier space can be written as

$$h_k'' + 2\mathcal{H}h_k' + k^2h_k = S\left(\vec{k},\tau\right), \tag{1.78}$$

where the source function $S\left(\vec{k},\tau\right)$ is given by

$$S\left(\vec{k},\tau\right)=4k^{2}\int\frac{d^{3}\vec{p}}{\left(2\pi\right)^{3/2}}\delta\sigma_{\vec{k}}\left(\tau\right)\delta\sigma_{\vec{k}-\vec{p}}\left(\tau\right)e^{lm}\left(\vec{k}\right)p_{l}p_{m} \tag{1.79}$$

where e^{lm} is a polarization tensor in a circular basis [18]. The solution to this equation is

$$h_{k}\left(\tau\right)=\frac{1}{a\left(\tau\right)}\int d\tau' g_{k}\left(\tau',\tau\right)a\left(\tau'\right)S\left(\vec{k},\tau\right), \tag{1.80}$$

where $g_{k}\left(\tau',\tau\right)$ is the Green function. We can write the perturbation of the curvaton field in terms of the transfer function and the primordial perturbation [18]

$$\delta\sigma_{k}\left(\tau\right)=T_{\sigma}\left(k,\tau\right)\delta\sigma_{k}, \tag{1.81}$$

with the primordial power spectrum

$$\left\langle \delta\sigma_{k}\delta\sigma_{q}\right\rangle =\frac{2\pi^{2}}{k^{3}}\delta^{(3)}\left(\vec{k}+\vec{q}\right)P_{\delta\sigma}\left(k\right). \tag{1.82}$$

The second-order tensor perturbations are produced when a given mode k enters the horizon and ends when the curvaton decays. Assuming that a mode k reenters the horizon during radiation dominated epoch, the Hubble rate is $H=1/\tau$ and so a given mode k enters the horizon at a time $\tau_{k}=1/k$. Denoting the mode which enters the horizon at the time of the curvaton decay as k_{D}, we can write

$$k_{D}=a\left(\tau_{D}\right)\Gamma, \tag{1.83}$$

where Γ is the decay rate of the curvaton and the scale factor is

$$a\left(\tau\right)=\frac{k_{D}^{2}}{\Gamma}\tau. \tag{1.84}$$

The zero mode of the curvaton field $\overline{\sigma}$ begins to oscillate at

$$\tau_{m}=\frac{1}{k_{D}}\left(\frac{\Gamma}{m}\right)^{1/2}, \tag{1.85}$$

where m is the curvaton mass. We consider the modes which enter the horizon when the zero mode $\overline{\sigma}$ is already oscillating

$$k\leq\left(\frac{m}{\Gamma}\right)^{1/2}k_{D}. \tag{1.86}$$

For this range of wavenumbers, $\delta\sigma_{k}\left(\tau\right)\approx\overline{\sigma}\approx a^{-3/2}$. Therefore we can write

$$\delta\sigma_{k}\left(\tau\right)=\left(\frac{\delta\sigma_{k}}{\overline{\sigma_{*}}}\right)\left(\frac{1}{k_{D}\tau}\right)^{3/2}\overline{\sigma}_{D}\simeq\frac{\zeta_{k}}{r}\left(\frac{1}{k_{D}\tau}\right)^{3/2}\overline{\sigma}_{D}, \tag{1.87}$$

where $\overline{\sigma}_{D}$ is the value of the zero mode of the curvaton field at the decay time. The GW energy density today then is given by [18]

$$\Omega_{GW} \simeq 10^{-15} \left(\frac{f_{NL}}{10^2}\right)^2 \left(\frac{k}{k_D}\right)^5 \left(\frac{\Gamma}{m}\right)^{7/2}, \tag{1.88}$$

for the range of wavenumbers

$$k_D \leq k \leq \left(\frac{m}{\Gamma}\right)^{1/2} k_D. \tag{1.89}$$

The maximum GW amplitude in the perturbative regime $\Gamma \leq m$, which also satisfies the constraints on NG from the CMB anisotropies, is of the order $\Omega_{\rm GW} \approx 10^{-15}$, which is above the sensitivity of interferometers like BBO and DECIGO.

1.2 Phase transitions

First-order phase transition in the early universe can give rise to a significant SGWB. The electroweak phase transition in the Standard Model is a cross-over, so it does not result in any considerable GW emission [51]. On the other hand, various extensions of the Standard Model predict strong first-order phase transitions that can produce a detectable GW signal [10].

During the first order phase transition, a potential barrier of the order parameter appears separating the symmetric false vacuum and symmetry-breaking true one that is more energetically favorable with decreasing temperature. The scalar field can pass from the false to the true vacuum either through quantum tunneling or thermal fluctuations. These processes occur through the nucleation of true vacuum bubbles in the background spacetime, which is still in a false vacuum. Due to the pressure acting on the bubble walls, the bubbles expand and, as a result, the free energy contained in the false vacuum is released. If the phase transition takes place in a vacuum, the released energy is converted only into gradient energy of the bubble walls, which can accelerate up to the speed of light. If the phase transition takes place in the primordial plasma and the field driving the phase transition is coupled to other fields in the surrounding plasma, most of the released energy is converted into the kinetic energy of the fluid [34].

At the end of the phase transition, the true vacuum bubbles collide breaking a spherical symmetry of bubble walls and creating non-zero anisotropic stress, which leads to the generation of GWs. [52].

A relevant parameter for the GW spectrum is T_*, the temperature of the thermal bath at the time t_* when GWs are produced. If there is no significant reheating, then it is approximately equal to the nucleation temperature $T_* \approx T_n$. The nucleation temperature is the temperature at which the probability that one bubble is nucleated per Hubble volume is of order 1. The bubble nucleation rate is [53]

$$\Gamma(t) = A(t)\, e^{-S(t)}, \tag{1.90}$$

where $S(t)$ is the Euclidean action of a critical bubble. It is given by either $O(4)$-symmetric solution for phase transitions in a vacuum or by $O(3)$-symmetric solution for

phase transitions at finite temperature. The inverse time duration of the phase transition β can be defined as the rate of variation of the bubble nucleation rate [10]

$$\beta = -\frac{\mathrm{d}S}{\mathrm{d}T} \simeq \frac{\dot{\Gamma}}{\Gamma}. \tag{1.91}$$

Another important parameter for the phase transitions is the ratio β/H_*. The smaller β/H_* is, the stronger the phase transition and therefore the GW signal. The ratio can be expressed as

$$\frac{\beta}{H_*} = T_* \frac{\mathrm{d}S}{\mathrm{d}T}. \tag{1.92}$$

The strength of the phase transition is characterized by the ratio of the vacuum energy density released in the phase transition to the energy density of the radiation bath at the moment of phase transition

$$\alpha = \frac{\rho_{vac}}{\rho^*_{rad}}, \tag{1.93}$$

where $\rho^*_{rad} = g_* \pi^2 T_*^4/30$, and g_* is the number of relativistic degrees of freedom at T_*. We also denote the bubble wall velocity in the rest frame far away from the bubble as v_w. Other relevant parameters are the fraction of vacuum energy that gets converted into gradient energy of the Higgs-like field, and into the bulk motion of the fluid respectively [54]

$$k_v = \frac{\rho_v}{\rho_{rad}} \quad k_\phi = \frac{\rho_\phi}{\rho_{rad}}. \tag{1.94}$$

The anisotropic stress sourcing the tensor perturbations are not correlated for wave numbers smaller than the Hubble radius at the time of production $k < a_* H_*$, because the causal processes that generate GWs cannot operate on scales larger than the horizon. At sub-horizon scales, the GW spectrum is determined by the details of the phase transition.

1.2.1 Contribution to the SGWB from the scalar field

The GW contribution due to the collision of the bubble walls is estimated using the envelope approximation [55, 56]. In this approximation, the energy is largely stored in the envelope of uncollided shells of the bubbles. Therefore the overlap regions of bubbles are neglected and the GWs are sourced only by the uncollided envelopes of bubbles. Numerical simulations result in the following GW spectrum [57]

$$\Omega_\phi h^2 \approx 1.610^{-5} \left(\frac{H_*}{\beta}\right)^2 \left(\frac{k_\phi \alpha}{1+\alpha}\right)^2 \left(\frac{100}{g_*(T_*)}\right)^{1/3} \left(\frac{0.11 v_w^3}{0.42 + v_w^2}\right) \frac{3.8 \left(\frac{f}{f_\phi}\right)^{2.8}}{1 + 2.8 \left(\frac{f}{f_\phi}\right)^{3.8}}, \tag{1.95}$$

where the peak frequency f_ϕ is determined by the duration of the phase transition

$$\frac{f_*}{\beta} = \frac{0.62}{1.8 - 0.1v_w + v_w^2}, \tag{1.96}$$

which is then redshifted and its value today is

$$f_\phi = 16.5 \times 10^{-3} mHz \left(\frac{f_*}{\beta}\right) \left(\frac{\beta}{H_*}\right) \left(\frac{T_*}{100GeV}\right) \left(\frac{g_*}{100}\right)^{1/6}. \tag{1.97}$$

1.2.2 Contribution to the SGWB from the sound waves

The expansion of bubbles can induce the compressional modes, namely the sound waves in the surrounding plasma due to the coupling of the scalar field with the surrounding plasma. When bubbles collide, the sound waves give rise to non-zero anisotropic stress generating GWs. Numerical simulations show that the sound waves can act as a source of GW long after the collision of the bubble walls. The GW signal from the sound waves is enhanced by a factor β/H_* due to the long-lasting nature of the sound waves[10]. The GW spectrum from sound waves from the numerical simulations is given by [58]

$$\Omega_{SW} h^2 \approx 2.610^{-6} \left(\frac{H_*}{\beta}\right) \left(\frac{k_v \alpha}{1+\alpha}\right)^2 \left(\frac{100}{g_*(T_*)}\right)^{1/3} v_w \left(\frac{f}{f_{SW}}\right)^3 \left(\frac{7}{4+3\left(\frac{f}{f_{SW}}\right)^2}\right)^{\frac{7}{2}}, \tag{1.98}$$

where the peak frequency is given by the characteristic size of the bubbles at the end of the phase transition

$$f_{SW} \simeq \frac{2}{\sqrt{3}} \frac{\beta}{v_w}, \tag{1.99}$$

that is redshifted and becomes

$$f_{SW} \simeq 1.9 \times 10^{-2} mHz \frac{1}{v_w} \left(\frac{\beta}{H_*}\right) \left(\frac{T_*}{100GeV}\right) \left(\frac{g_*}{100}\right)^{1/6}. \tag{1.100}$$

1.2.3 Contribution to the SGWB from MHD turbulence

The collisions of the bubble walls are also expected to give rise to the magneto-hydrodynamic (MHD) turbulence, which can generate GWs due to the anisotropic stresses of the chaotic fluid motions and the magnetic field since the primordial plasma is fully ionized. For Kolmogorov type turbulence [59] the contribution to the GW spectrum from MHD turbulence is [60]

$$\Omega_{turb}h^2 \approx 3.35\times10^{-4}\left(\frac{H_*}{\beta}\right)\left(\frac{k_{turb}\alpha}{1+\alpha}\right)^{\frac{3}{2}}\left(\frac{100}{g_*(T_*)}\right)^{1/3} v_w \frac{\left(\frac{f}{f_{turb}}\right)^3}{(1+\left(\frac{f}{f_{turb}}\right)^{\frac{11}{3}})(1+8\pi f H_*)}, \tag{1.101}$$

where $k_{turb}=\epsilon k_v$ is the fraction of bulk kinetic energy related to the vortical motion. The GWs from the MHD turbulence will also be amplified by a factor β/H_* since the MHD turbulence is a long-lasting source of GWs, which takes several Hubble times to dissipate [60]. Similarly to the sound waves, the peak frequency is related to the inverse characteristic length scale of the source, namely the bubble size at the end of the phase transition

$$f_{turb} \simeq \frac{3.5}{2}\frac{\beta}{v_w}, \tag{1.102}$$

which after redshifting becomes

$$f_{turb} \simeq 2.7\times10^{-2} mHz \frac{1}{v_w}\left(\frac{\beta}{H_*}\right)\left(\frac{T_*}{100GeV}\right)\left(\frac{g_*}{100}\right)^{1/6}. \tag{1.103}$$

1.2.4 Dynamics of the Phase Transition

The relative contribution of each process that generates the GWs strongly depends on the details of the phase transition. It is crucial whether the bubble wall reaches a terminal velocity or not. The bubble wall velocity v_w comes from the balance of the pressure forcing the bubble to expand and the friction force due to the interaction of the bubble wall with the plasma, which slows down the expansion [10]. If the phase transition occurs in a thermal plasma and the friction is high, the bubble wall reaches a terminal velocity. In this case, the energy of the scalar field is negligible and the dominant contributions to the GW signal are the sound waves and MHD turbulence. The total contribution to the GW signal can be approximated as

$$\Omega_{GW}h^2 \approx \Omega_{SW}h^2 + \Omega_{turb}h^2. \tag{1.104}$$

The efficiency factor k_v in the limits of small and large v_w is given by [10]

$$k_v \simeq \begin{cases} \alpha\left(0.73+0.083\sqrt{\alpha}+\alpha\right)^{-1} & v_w \sim 1 \\ v_w^{6.5} 6.9\alpha\left(1.36-0.037\sqrt{\alpha}+\alpha\right)^{-1} & v_w \leq 1 \end{cases} \tag{1.105}$$

The GW spectrum for this scenario is shown in Figure 1.2, for fixed T_*,α and v_w, and varying β/H_*. We set $\epsilon=0.05$, therefore the sound waves provide the dominant contribution. Turbulence is important at high frequencies since the sound waves decay faster. When β/H_* increases, the peak of the signal shifts towards larger frequencies, and the overall amplitude decreases. Due to the factor, $8\pi f/H_*$ the contribution from turbulence is suppressed.

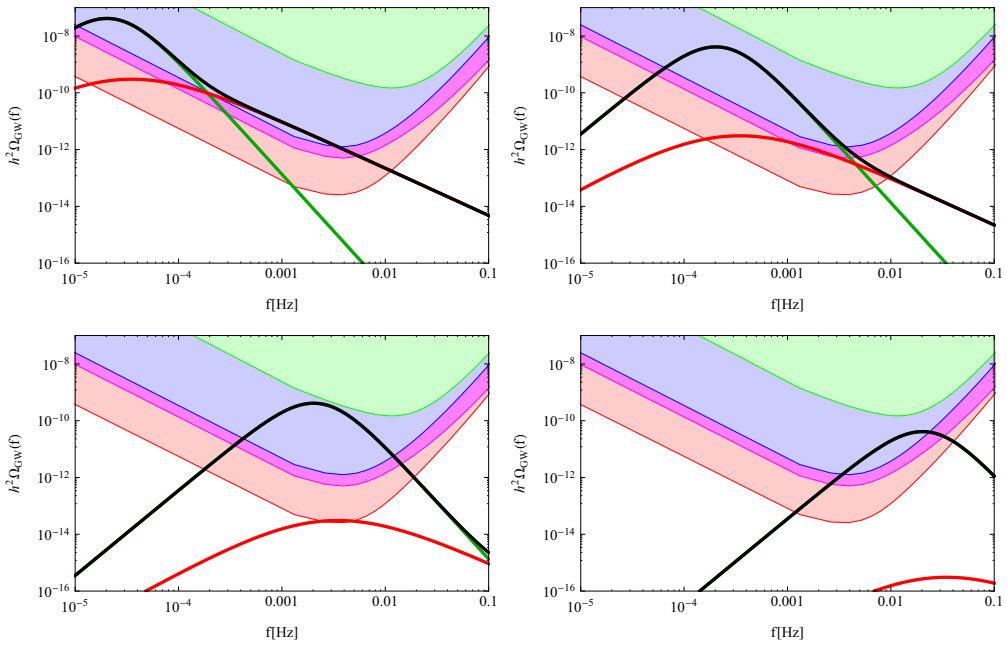

Figure 1.2: GW spectra for $T_* = 100GeV, \alpha = 0.5, v_w = 0.95$ and varying β/H_* from top left to bottom right, $\beta/H_* = 1$, $\beta/H_* = 10$, $\beta/H_* = 100$, $\beta/H_* = 100$. The black line denotes the total GW spectrum, the green line is the contribution from sound waves, and the red line is the contribution from MHD turbulence. The shaded areas represent the different LISA configurations [10].

Alternatively, if the bubble wall velocity can accelerate without bound and reach the speed of light [61], a further difference is whether plasma effects are negligible or not. If the bubble walls are expanding in a thermal plasma, then the scalar field contribution cannot be neglected, since it dominates for $\alpha \gg 1$. The total GW spectrum can be approximated as

$$\Omega_{GW}h^2 \approx \Omega_\phi h^2 + \Omega_{SW}h^2 + \Omega_{turb}h^2. \tag{1.106}$$

When α increases, the wall velocity rapidly becomes relativistic. We denote a_∞ as the minimum value of a such that the bubble wall velocity can reach the speed of light [62]. Above this value, the surplus energy goes into accelerating the bubble wall. This surplus energy can be written in terms of the fraction

$$k_\phi = \frac{\alpha - \alpha_\infty}{\alpha} \geq 0. \tag{1.107}$$

Only the fraction α_∞/α is transformed into bulk motion and thermal energy. From

eq. (1.105) we can write

$$k_v = \frac{\alpha_\infty}{\alpha} k_\infty, \tag{1.108}$$

where

$$k_\infty = \frac{\alpha_\infty}{0.73 + 0.083\sqrt{\alpha_\infty} + \alpha_\infty}. \tag{1.109}$$

The parameter α_∞ is model-dependent. For electroweak phase transitions in models with Standard Model particle content, it can be written as

$$a_\infty \simeq 4.9 \times 10^{-3} \left(\frac{\phi_*}{T_*}\right)^2. \tag{1.110}$$

The GW spectrum for this scenario is shown in Figure 1.3, for fixed T_*,α and v_w, and varying β/H_*. If the ratio β/H_* is small, then the scalar field contribution can dominate the GW spectrum, since the enhancement of the signal by a factor β/H_* is less important.

If there is a significant amount of supercooling, the phase transition essentially occurs in a vacuum. The friction is low, therefore the effects of the plasma are negligible and the bubble wall speed can readily accelerate reaching the speed of light. Most of the energy goes into the gradient energy of the Higgs-like field. The total GW, in this case, can be approximated as

$$\Omega_{GW} h^2 \approx \Omega_\phi h^2. \tag{1.111}$$

We can approximate $k_\phi \simeq 1$ and $v_w \simeq 1$. The temperature of the thermal bath at the time of GW production is approximately equal to the reheating temperature $T_* \simeq T_{reh}$. So far we have assumed that the phase transition occurs without a significant reheating, therefore $T_* \simeq T_n \simeq T_{reh}$. In the vacuum case, it is instead expected, $T_n \ll T_{reh} \simeq T_*$, and the definitions of β/H_* and α are altered

$$\frac{\beta}{H_*} = \frac{H(T_n)}{H_*} T_n \frac{\mathrm{d}S}{\mathrm{d}T}, \tag{1.112}$$

$$\alpha = \frac{\rho_{vac}}{\rho_{rad}(T_n)}. \tag{1.113}$$

In case, if reheating is fast $H(T_n) \simeq H_*$ despite that $T_n \ll T_*$. Since $\alpha \gg 1$ the dependence of GW spectrum on α drops.

1.3 Cosmic strings

Cosmic strings are one-dimensional topological defects produced as a result of a symmetry-breaking phase transition in the early universe. Cosmic strings may arise at

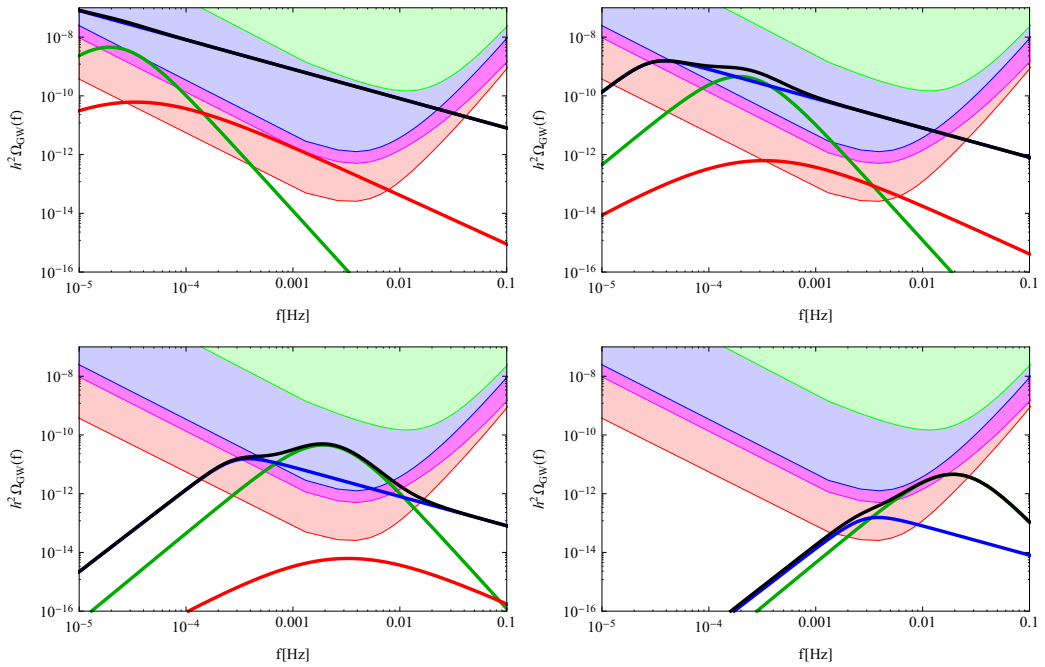

Figure 1.3: GW spectra for $T_* = 100GeV, \alpha = 1, v_w = 1, \alpha_\infty = 0.3$ and varying β/H_* from top left to bottom right, $\beta/H_* = 1$, $\beta/H_* = 10$, $\beta/H_* = 100$, $\beta/H_* = 100$. The black line denotes the total GW spectrum, the blue line the contribution from the scalar field, the green line the contribution from sound waves, and the red line the contribution from MHD turbulence. The shaded areas represent the different LISA configurations[10].

the end of inflation in supersymmetric GUT models of Hybrid inflation [19] or they may be the fundamental superstrings produced at the end of brane inflation [20].

The linear energy of a string is μ, which in the Nambu-Goto theory corresponds to the string tension. It can be expressed as the dimensionless quantity $G\mu$, where G is Newton's constant. In the case of standard field theory strings, the string tension is related to the vacuum expectation value ν of the ordering field in the phase transition through [34]

$$G\mu = \pi \left(\frac{\nu}{m_{Pl}} \right)^2 \tag{1.114}$$

A network of cosmic strings is stretched by the cosmological expansion, which leads to intersections between them. When strings cross each other, they reconnect forming the string loops. Loops with a diameter smaller than the horizon begin to oscillate under their tension and decay emitting GWs. Besides the sub-horizon loops, there are long strings that stretch on superhorizon scales and can generate GWs. However, the

sub-horizon cosmic string loops provide the dominant contribution to the GW signal. Besides the stationary GW background, also strong infrequent GW bursts are possible. They are emitted by cusps, associated with points where the string briefly reaches the speed of light, and kinks, related to discontinuities on the tangent vector of the string. However, we will focus on the stationary GW background from the decaying loops. The network of cosmic strings evolves toward an attractor scaling solution in which its energy density is a fraction of the background energy density.

To compute the GW spectrum generated by a network of cosmic strings we must introduce the number density of cosmic string loops $n\left(l,t\right)$ and the power emitted by a cosmic string loop $P_{GW}\left(f,l\right)$.

The number density of cosmic string loops $n\left(l,t\right)$ of length l at time t can be estimated through numerical simulations. Simulations run only over a finite time interval, therefore to extrapolate the results to any moment in the evolution of the network, the scaling of loops is vital. It implies that [11]

$$n\left(l,t\right)=t^{-4}n\left(x\right), \tag{1.115}$$

where $x=l/t$ is the ratio of the size of the loop to roughly the horizon scale. We also introduce the loop production function $f\left(l,t\right)$, which is the number density of non-self-intersecting loops of lengths between l and $l+dl$ produced per unit time, per unit volume, which scales as

$$f\left(l,t\right)=t^{-5}f\left(x\right). \tag{1.116}$$

The number density of loops then is obtained by integrating the loop production function

$$n\left(l,t\right)=\int dt'f\left(l',t'\right)\left(\frac{a\left(t'\right)}{a\left(t\right)}\right)^{3}. \tag{1.117}$$

The length of the loop is given by

$$l=l'+\Gamma G\mu\left(t'-t\right), \tag{1.118}$$

where Γ is the dimensionless constant characterizing the efficiency of the energy loss mechanism [34]. If the scale factor can be written as $a\left(t\right)\approx t^{\nu}$, the loop number density is given by

$$n\left(x\right)=\frac{1}{\left(x+\Gamma G\mu\right)^{3(1-\nu)+1}}\int_{x}^{\infty}\left(x'+\Gamma G\mu\right)^{3(1-\nu)}f\left(x'\right)dx', \tag{1.119}$$

In the radiation-dominated era, the scaling number density of loops from simulations is given by [63]

$$n\left(x\right)=\frac{0.18}{\left(x+\Gamma G\mu\right)^{5/2}}, \tag{1.120}$$

with a cutoff at the maximum size of a loop, $x = l/t = 0.1$. It then follows from eq. (1.115) that

$$n(l,t) = \frac{0.18}{t^{3/2}(x+\Gamma G\mu)^{5/2}}, \tag{1.121}$$

with $l \leq 0.1t$, the form of the loop production function was found numerically.

A cosmic string loop oscillates under its tension and emits GWs in a series of harmonics modes. The energy radiated in GWs into each harmonic mode is given by [34]

$$\dot{E}_{GW}^{(n)} = P_n \Gamma G\mu^2, \tag{1.122}$$

where P_n is the fraction of energy emitted per harmonic mode n with $\sum_{n=1}^{\infty} P_n = 1$, so that $\dot{E}_{GW} = \sum_{n=1}^{\infty} \dot{E}_{GW}^{(n)} = \Gamma G\mu^2$ It can be parameterized in terms of a spectral index q as

$$P_n = \frac{D_q}{n^{q+1}}. \tag{1.123}$$

Given the condition $\sum_{n=1}^{\infty} P_n = 1$, we find

$$D_q = \frac{1}{\zeta(q+1)}, \tag{1.124}$$

where $\zeta(q)$ is a Riemann zeta function. We can approximate the sum of discrete modes in a continuous one

$$\sum_{n=1}^{\infty} P_n \simeq l \int df P(f), \tag{1.125}$$

where

$$P(f) = \frac{C_q}{(fl)^{q+1}}, \tag{1.126}$$

with the normalization constant C_q fixed to satisfy the continuum normalization condition $l \int df P(f) = 1$. We introduce P_{GW}, namely the total energy emitted by a cosmic string loop of length l in GWs within the frequency range $[f, f+df)$

$$dP_{GW}(f) = \Gamma G\mu^2 l P(f)\, df. \tag{1.127}$$

It follows that the GW energy density emitted by loop of the length in the interval $[l, l+dl)$ and within the frequency range $[f, f+df)$ during the time interval $[t, t+dt)$ is

$$d\rho_{GW} = dP_{GW}(f)\, dt n(l,t)\, dl. \tag{1.128}$$

Taking into account that the energy density redshifts as $1/a^4$ and the frequency today is related to those at emission by $f = f_e a_e/a_0$, the GW energy density reads

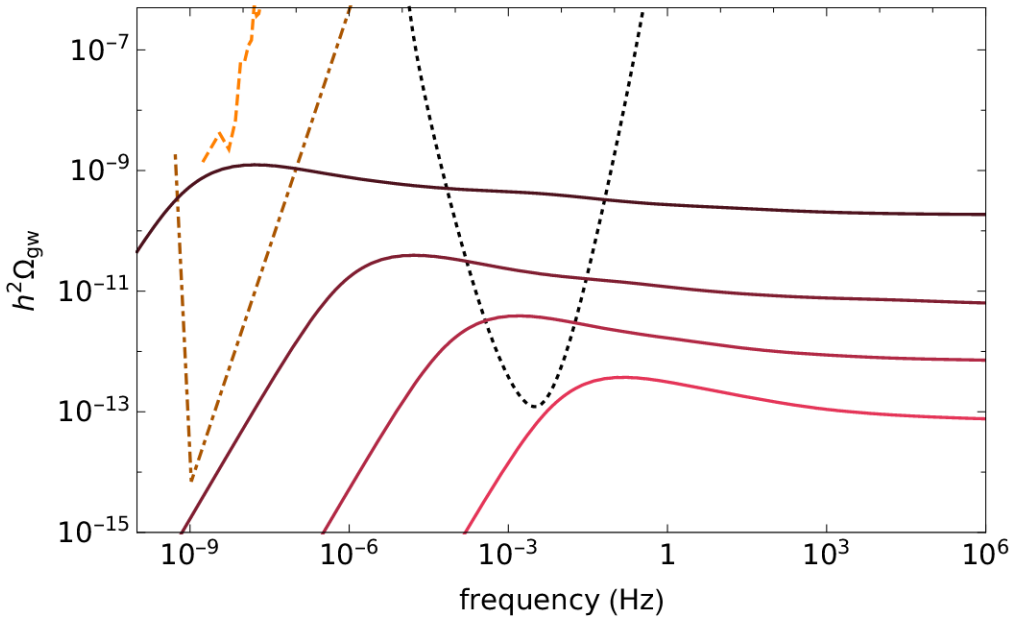

Figure 1.4: Cosmic string SGWB for different values of $G\mu$. The dark red curve is for $G\mu = 10^{-13}$. The light red curve is for $G\mu = 10^{-17}$. The dashed orange curve is the EPTA sensitivity. The dash-dotted dark orange curve is the (projected) SKA sensitivity. The dotted black curve is the LISA sensitivity [11].

$$d\rho^{(0)}(t) = \left(\frac{a(t)}{a_0}\right)^4 d\rho(t) = \left(\frac{a(t)}{a_0}\right)^3 \Gamma G\mu^2 l P\left(a_0/a(t) f l\right) n(l,t)\, dl df dt, \tag{1.129}$$

integrating the GW spectrum from the emission time t_* until today t_0, we find

$$\frac{\mathrm{d}\rho^{(0)}}{\mathrm{d}f} = \Gamma G\mu^2 \int_{t_*}^{t_0} dt \left(\frac{a(t)}{a_0}\right)^3 \int_0^{\alpha/H(t)} dl\, ln(l,t)\, P\left(\frac{a_0}{a(t)} f l\right). \tag{1.130}$$

At last, we can write the GW spectrum given by the superposition of the GW harmonics emitted by the distribution of loops through cosmic history

$$\Omega_{GW} h^2 = \frac{1}{\rho_c}\frac{\mathrm{d}\rho_{GW}}{\mathrm{d}lnf} = \frac{\Gamma G\mu^2 f}{\rho_c} \int_{t_*}^{t_0} dt \left(\frac{a(t)}{a_0}\right)^3 \int_0^{\alpha/H(t)} dl\, ln(l,t)\, P\left(\frac{a_0}{a(t)} f l\right). \tag{1.131}$$

Figure 1.4 depicts the SGWB from the network of cosmic strings for different values of $G\mu$. The GW spectrum becomes flat at very high frequencies. It depends only on the average total power emitted by a loop and the total number of loops. It follows that

$$\Omega_{GW}^{plateau} \approx 8.04 \Omega_{rad} \sqrt{\frac{G\mu}{\Gamma}}. \tag{1.132}$$

One of the most important consequences of this is that in a high-frequency regime the GW amplitude depends only on $G\mu$ and Γ. It does not depend on the particular form of the loop power spectrum.

The constraints on the cosmic string tension $G\mu$ depend on several parameters describing the loop production size and the number density. Currently, the constraint on the string tension $G\mu$ from the CMB data obtained by the Planck Satellite is $G\mu \leq 1.6 \times 10^{-7}$ [64]. It is possible to find the lowest value of string tension $G\mu$ for which the amplitude is above the LISA sensitivity. The exact bound depends on the choice of model and P_n, but in the range of frequencies that LISA will be able to probe its value is of the order $O\left(10^{-17}\right)$ [11].

Chapter 2

Stochastic Gravitational Wave Background anisotropies

2.1 Boltzmann equation for GW

To study the angular anisotropies in the GW energy density we use a Boltzmann approach in analogy with the CMB anisotropies [22, 23, 24]. We can define a graviton distribution function $f = f\left(\eta, x^i, q, n^i\right)$, which is function of position x^μ and momentum $p^\mu = dx^\mu/d\lambda$, where λ is an affine parameter along the GW trajectory. The Boltzmann equation for the graviton distribution function is

$$L\left[f\right] = C\left[f\right] + I\left[f\right], \tag{2.1}$$

where $L\left[f\right] = df/d\lambda$ is the Liouville operator, $C\left[f\right]$ and $J\left[f\right]$ accounts for the collision of GWs, and for their emissivity from cosmological and astrophysical sources respectively [14].

We consider a perturbed spatially flat FRW metric in the Poisson gauge [25]

$$ds^2 = a^2(\eta)\left[-e^{2\Phi}d\eta^2 + \left(e^{-2\Psi}\delta_{ij} + \chi_{ij}\right)dx^i dx^j\right], \tag{2.2}$$

where $a(\eta)$ is the scale-factor, Φ and Ψ are the scalar perturbations and χ_{ij} are the transverse-traceless tensor perturbations. We neglect vector perturbations at first order.

The collision of GWs has an impact on the graviton distribution only at higher order, therefore at the first order in perturbations, then $C\left[f\right] = 0$. The source of emissivity can be of astrophysical origins, such as black hole merging, or cosmological origins, such as inflation. Since we are interested only in the SGWB from cosmological sources, therefore we consider the emissivity term as the initial condition and so $I\left[f\right] = 0$. This leads to the free Boltzmann equation

$$\frac{\mathrm{d}f}{\mathrm{d}\eta} = \frac{\partial f}{\partial \eta} + \frac{\mathrm{d}x^i}{\mathrm{d}\eta}\frac{\partial f}{\partial x^i} + \frac{\mathrm{d}q}{\mathrm{d}\eta}\frac{\partial f}{\partial q} + \frac{\mathrm{d}n^i}{\mathrm{d}\eta}\frac{\partial f}{\partial n^i} = 0. \tag{2.3}$$

where $n^i = \hat{p}$ is the direction along the GW trajectory. We have used a comoving momentum $q = |\vec{p}|a$ instead of the physical one, which simplifies the equations by factoring out the expansion of the universe. The first two terms represent a free streaming term, namely the propagation of GWs at all scales. The third term encodes the redshifting of gravitons, while the fourth term represents the effect of gravitational lensing and is of the second order, so we can disregard this term at the first order.

Gravitons, similarly to photons, propagate along null geodesics defined by the background metric. Considering that gravitons are massless particles, then

$$p^2 = g_{\mu\nu} p^\mu p^\nu = 0, \tag{2.4}$$

then

$$-a^2 e^{2\Phi} \left(p^0\right)^2 + p^2 = 0. \tag{2.5}$$

We can write the three-momentum as

$$p^2 = g_{ij} p^i p^j, \tag{2.6}$$

where $p^i = A n^i$, then we can write

$$p^0 = \frac{q}{a^2} e^{-\Phi}, \tag{2.7}$$

and

$$p^i = \frac{q}{a^2} n^i e^{\Psi} \left(1 - \frac{1}{2} \chi_{jk} n^j n^k\right). \tag{2.8}$$

Thus we can write

$$\frac{\mathrm{d}x^i}{\mathrm{d}\eta} = \frac{p^i}{p^0} = n^i e^{\Phi+\Psi} \left(1 - \frac{1}{2} \chi_{jk} n^j n^k\right). \tag{2.9}$$

To express the third term in eq. (2.3) we use the geodesic equations

$$\frac{\mathrm{d}p^\mu}{\mathrm{d}\lambda} = -\Gamma^\mu_{\nu\tau} p^\nu p^\tau. \tag{2.10}$$

The derivative with respect to λ can be rewritten as a derivative with respect to conformal time η

$$\frac{\mathrm{d}p^0}{\mathrm{d}\eta} = -\frac{\Gamma^0_{\nu\tau} p^\nu p^\tau}{p^0}, \tag{2.11}$$

using eq. (2.8) we can write

$$\frac{q}{a^2} \left(-2\mathcal{H} - \frac{\mathrm{d}\Phi}{\mathrm{d}\eta} + 2\mathcal{H}\Phi\right) + \frac{1-\Phi}{a^2} \frac{\mathrm{d}q}{\mathrm{d}\eta} = \Gamma^0_{\nu\tau} p^\nu p^\tau \frac{a^2}{q} (1+\Phi), \tag{2.12}$$

then

$$\frac{\mathrm{d}q}{\mathrm{d}\eta} = q\left(\frac{\mathrm{d}\Phi}{\mathrm{d}\eta} + 2\mathcal{H}\right) - \Gamma^0_{\nu\tau}p^\nu p^\tau \frac{a^4}{q}\left(1+2\Phi\right), \tag{2.13}$$

reexpressing $\frac{\mathrm{d}\Phi}{\mathrm{d}\eta}$ in terms of partial derivatives

$$\frac{\mathrm{d}q}{\mathrm{d}\eta} = q\left(\frac{\partial\Phi}{\partial\eta} + n^i\frac{\partial\Phi}{\partial x^i} + 2H\right) - \Gamma^0_{\nu\tau}p^\nu p^\tau \frac{a^4}{q}\left(1+2\Phi\right), \tag{2.14}$$

making the second term explicit

$$\Gamma^0_{\nu\tau}p^\nu p^\tau = \left(1+2\Phi\right)\frac{q^2}{a^4}\left(-\frac{\partial\Phi}{\partial\eta} - 2n^i\frac{\partial\Phi}{\partial x^i} + \frac{\partial\Psi}{\partial\eta} - 2H - \frac{1}{2}\frac{\partial\chi_{jk}}{\partial\eta}n^j n^k\right). \tag{2.15}$$

Finally, we have

$$\frac{\mathrm{d}q}{\mathrm{d}\eta} = q\left(\frac{\partial\Psi}{\partial\eta} - n^i\frac{\partial\Phi}{\partial x^i} - \frac{1}{2}\frac{\partial\chi_{jk}}{\partial\eta}n^j n^k\right). \tag{2.16}$$

Inserting these terms into eq. (2.3) leads to

$$\frac{\partial f}{\partial\eta} + n^i\frac{\partial f}{\partial x^i} + \left(\frac{\partial\Psi}{\partial\eta} - n^i\frac{\partial\Phi}{\partial x^i} - \frac{1}{2}\frac{\partial\chi_{jk}}{\partial\eta}n^j n^k\right)q\frac{\partial f}{\partial q} = 0. \tag{2.17}$$

The graviton distribution function f can be expanded as

$$f\left(\eta, x^i, q, n^i\right) = \overline{f}\left(q\right) + \delta f\left(\eta, x^i, q, n^i\right) = \overline{f}\left(q\right) - q\frac{d\overline{f}\left(q\right)}{dq}\Gamma\left(\eta, x^i, q, n^i\right), \tag{2.18}$$

where f is the leading, homogeneous and isotropic term and δf is a subdominant anisotropic contribution, parameterized in terms of the dimensionless function Γ. The two functions are the solutions of the Boltzmann equation at zeroth and first order respectively. The Boltzmann equation at zero order reads

$$\frac{\mathrm{d}\overline{f}}{\mathrm{d}\eta} = 0, \tag{2.19}$$

which is solved by the distribution, which is function only of the comoving momentum $f = \overline{f}\left(q\right)$. The physical graviton number density can be written as

$$n \propto \int d^3p\overline{f}\left(q\right) = \int \frac{d^3q}{a^3}\overline{f}\left(q\right) \propto \frac{1}{a^3}. \tag{2.20}$$

In the case of CMB photons, the distribution function is

$$\overline{f}_{CMB} \propto \frac{1}{e^{p/T}-1}, \tag{2.21}$$

where T is the temperature of the CMB bath and it follows that $\Gamma = \delta T/T$. Therefore the temperature anisotropies are frequency-independent up to the second order in the

perturbations, while for gravitons the collisional term is zero and so the function Γ can have an order one dependence on frequency.

The graviton distribution function is related to the GW energy density. The GW energy density can be expressed in terms of spectral energy density Ω_{GW} as

$$\rho_{\rm GW}\left(\eta, x^i\right) = \frac{1}{a_0^4}\int d^3q q\, f\left(\eta, x^i, q, n^i\right) = \rho_{crit,0}\int dlnq\, \Omega_{\rm GW}\left(x^i, q\right). \tag{2.22}$$

The homogeneous and isotropic component of $\Omega_{\rm GW}$ is

$$\overline{\Omega}_{\rm GW}\left(x^i, q\right) = \frac{4\pi}{\rho_{crit,0}}\frac{q^4}{a_0^4}\overline{f}\left(q\right). \tag{2.23}$$

We define the full spectral GW energy density $\Omega_{\rm GW}$ as

$$\Omega_{\rm GW} = \frac{1}{4\pi}\int d^2n^i w_{\rm GW}\left(x^i, q, n^i\right), \tag{2.24}$$

where d^2n^i is the surface area element on the unit sphere. We define the SGWB density contrast as

$$\delta_{\rm GW} = \frac{w_{\rm GW}\left(x^i, q, n^i\right) - \overline{\Omega}_{\rm GW}\left(q\right)}{\overline{\Omega}_{\rm GW}\left(q\right)} = -\frac{q}{\overline{f}}\frac{\partial\overline{f}}{\partial q}\Gamma, \tag{2.25}$$

using eq. (2.23) we have

$$\frac{q}{\overline{f}}\frac{\partial\overline{f}}{\partial q} = -4 + \frac{\partial\ln\overline{\Omega}_{GW}\left(q\right)}{\partial\ln q}, \tag{2.26}$$

then the SGWB density contrast is

$$\delta_{\rm GW} = \left[4 - \frac{\partial\ln\overline{\Omega}_{\rm GW}\left(q\right)}{\partial\ln q}\right]\Gamma. \tag{2.27}$$

It should be remarked that in contrast to photons, the initial graviton distribution is not thermal, therefore Γ, in general, can depend on q. To simplify the equation we introduce the spectral tilt defined as

$$n_T = \frac{\partial\ln\overline{\Omega}_{\rm GW}\left(q\right)}{\partial\ln q}. \tag{2.28}$$

Then we can write the GW density contrast as

$$\delta_{\rm GW} = \left[4 - n_T\right]\Gamma. \tag{2.29}$$

The Boltzmann equation in terms of the function Γ reads

$$\frac{\partial\Gamma}{\partial\eta} + n^i\frac{\partial\Gamma}{\partial x^i} = S\left(\eta, x^i, n^i\right), \tag{2.30}$$

where

$$S\left(\eta, x^i, n^i\right) = \frac{\partial \Psi}{\partial \eta} - n^i \frac{\partial \Phi}{\partial x^i} - \frac{1}{2}\frac{\partial \chi_{jk}}{\partial \eta} n^j n^k, \tag{2.31}$$

is the source function that encodes the effects due to scalar and tensor perturbations. It should be noted that the source function is frequency-independent, so the anisotropies due to the propagation through the scalar and tensor perturbations of the universe are frequency-independent at first order.

To solve this equation we use the Fourier transform in spatial coordinates

$$\Gamma\left(\eta, \vec{x}, q, \vec{n}\right) = \int \frac{d^3k}{(2\pi)^3} e^{i\vec{k}\cdot\vec{x}} \Gamma\left(\eta, k, q, \vec{n}\right), \tag{2.32}$$

then the Boltzmann equation can be written as

$$\Gamma' + ik\mu\Gamma = S\left(\eta, \vec{k}, \vec{n}\right), \tag{2.33}$$

where we define $\mu = \vec{k}\cdot\vec{n}$ as the cosine of the angle between the Fourier variable $\vec{k}$ and the direction along the GW trajectory. The source function in Fourier space reads

$$S\left(\eta, \vec{k}, \vec{n}\right) = \Psi' - ik\mu\Phi - \frac{1}{2}\chi'_{jk} n^j n^k. \tag{2.34}$$

The solution of the equation is [25]

$$\begin{aligned}\Gamma\left(\eta, \vec{k}, q, \vec{n}\right) = {} & e^{ik\mu(\eta_{in}-\eta)}\Gamma\left(\eta_{in}, \vec{k}, q, \vec{n}\right) + \\ & + \int_{\eta_{in}}^{\eta} d\eta' e^{ik\mu(\eta'-\eta)} \left[\frac{\partial \Psi\left(\eta', \vec{k}\right)}{\partial \eta'} - ik\mu\Phi\left(\eta', \vec{k}\right) - \frac{1}{2}\frac{\partial \chi_{jk}\left(\eta', \vec{k}\right)}{\partial \eta'} n^j n^k\right],\end{aligned} \tag{2.35}$$

integrating the second term in the second line by parts, we get

$$\begin{aligned}\Gamma\left(\eta, \vec{k}, q, \vec{n}\right) = {} & e^{ik\mu(\eta_{in}-\eta)}\left[\Gamma\left(\eta_{in}, \vec{k}, q, \vec{n}\right) + \Phi\left(\eta_{in}, \vec{k}\right)\right] - \Phi\left(\eta, \vec{k}\right) \\ & + \int_{\eta_{in}}^{\eta} d\eta' e^{ik\mu(\eta'-\eta)} \left[\frac{\partial\left[\Psi\left(\eta', \vec{k}\right) + \Phi\left(\eta', \vec{k}\right)\right]}{\partial \eta'} - \frac{1}{2}\frac{\partial \chi_{jk}\left(\eta', \vec{k}\right)}{\partial \eta'} n^j n^k\right].\end{aligned} \tag{2.36}$$

We can disregard $-\Phi(\eta', \vec{k})$, since the monopole term does not contribute to the anisotropy of SGWB, then

$$\begin{aligned}\Gamma\left(\eta,\vec{k},q,\vec{n}\right) &= \int_{\eta_{in}}^{\eta} d\eta' e^{ik\mu(\eta'-\eta)}\left[\left[\Gamma\left(\eta',\vec{k},q,\vec{n}\right)+\Phi\left(\eta',\vec{k}\right)\right]\delta\left(\eta_{in}-\eta'\right)\right. \\ &+ \left.\frac{\partial\left[\Psi\left(\eta',\vec{k}\right)+\Phi\left(\eta',\vec{k}\right)\right]}{\partial\eta'}-\frac{1}{2}\frac{\partial\chi_{jk}\left(\eta',\vec{k}\right)}{\partial\eta'}n^j n^k\right] \end{aligned} \tag{2.37}$$

The first term represents the initial condition. This term depends on the frequency q and, in general, it can also depend on $\vec{n}$, which is more general than the dependence on $\mu = \vec{k}\cdot\vec{n}$, but we focus on the statistically isotropic case, so we assume an initial condition of the form $\Gamma_{in} = \Gamma\left(\eta_{in},\vec{k},q\right)$.

2.2 Spherical harmonics decomposition

We divide the solution into three terms

$$\Gamma\left(\eta,\vec{k},q,\vec{n}\right) = \Gamma_I\left(\eta,\vec{k},q,\vec{n}\right)+\Gamma_S\left(\eta,\vec{k},\vec{n}\right)+\Gamma_T\left(\eta,\vec{k},\vec{n}\right), \tag{2.38}$$

where I, S, and T denote initial, scalar, and tensor terms respectively and correspond to

$$\begin{aligned}\Gamma_I\left(\eta,\vec{k},q,\vec{n}\right) &= e^{ik\mu(\eta_{in}-\eta)}\Gamma\left(\eta_{in},\vec{k},q\right), \\ \Gamma_S\left(\eta,\vec{k},\vec{n}\right) &= \int_{\eta_{in}}^{\eta} d\eta' e^{ik\mu(\eta'-\eta)}\left[\Phi\left(\eta',\vec{k}\right)\delta\left(\eta_{in}-\eta'\right)+\frac{\partial\left[\Psi\left(\eta',\vec{k}\right)+\Phi\left(\eta',\vec{k}\right)\right]}{\partial\eta'}\right], \\ \Gamma_T\left(\eta,\vec{k},\vec{n}\right) &= -\int_{\eta_{in}}^{\eta} d\eta' e^{ik\mu(\eta'-\eta)}\frac{1}{2}\frac{\partial\chi_{jk}\left(\eta',\vec{k}\right)}{\partial\eta'}n^j n^k. \end{aligned} \tag{2.39}$$

Similar to CMB, to compute the angular power the spectrum we decompose the solution in spherical harmonics

$$\Gamma\left(\vec{n}\right) = \sum_{\ell}\sum_{m=-\ell}^{\ell}\Gamma_{\ell m}Y_{\ell m}\left(\vec{n}\right), \quad \text{where} \quad \Gamma_{\ell m} = \int d^2n\,\Gamma\left(\vec{n}\right)\,Y^*_{\ell m}\left(\vec{n}\right), \tag{2.40}$$

and then we have

$$\begin{aligned}\Gamma_{\ell m} &= \int d^2n Y^*_{\ell m}\left(\vec{n}\right)\int\frac{d^3k}{\left(2\pi\right)^3}e^{i\vec{k}\vec{x}}\left[\Gamma_I\left(\eta,\vec{k},q,\vec{n}\right)+\Gamma_S\left(\eta,\vec{k},\vec{n}\right)+\Gamma_T\left(\eta,\vec{k},\vec{n}\right)\right] \\ &= \Gamma_{\ell m,I}+\Gamma_{\ell m,S}+\Gamma_{\ell m,T}. \end{aligned} \tag{2.41}$$

2.2.1 Initial condition term

First, we evaluate the initial condition term

$$\Gamma_{\ell m,I} = \int \frac{d^3k}{(2\pi)^3} e^{i\vec{k}\vec{x_0}} \Gamma\left(\eta_{in}, \vec{k}, q\right) \int d^2n Y^*_{\ell m}\left(\vec{n}\right) e^{-ik\mu(\eta_0-\eta_{in})} \tag{2.42}$$

as for CMB anisotrpies [26], we exploit the identity

$$e^{i\vec{x}\vec{y}} = 4\pi \sum_{\ell} \sum_{m=-\ell}^{\ell} (-i)^{\ell} j_l\left(xy\right) Y_{\ell m}\left(\hat{x}\right) Y^*_{\ell m}\left(\hat{y}\right), \tag{2.43}$$

and obtain

$$\Gamma_{\ell m,I} = 4\pi (-i)^{\ell} \int \frac{d^3k}{(2\pi)^3} e^{i\vec{k}\vec{x_0}} \Gamma\left(\eta_{in}, \vec{k}, q\right) Y^*_{\ell m}\left(\vec{k}\right) j_{\ell}\left(k\left(\eta_0 - \eta_{in}\right)\right). \tag{2.44}$$

where $\vec{x}_0$ denotes the location of the observer, which could be taken as the origin, η_0 is the present time, and η_{in} is the initial time. The initial condition term arises when the GWs are generated, therefore it depends on the specific mechanism of the GW production.

2.2.2 Scalar sourced term

The scalar term arises during the propagation of GWs through the large-scale perturbations of the universe and therefore is model-independent. The scalar perturbations can be expressed in terms of a transfer function, which describes the time dependence of the perturbations from the time of production till today, and a stochastic variable ζ [26]. The statistical properties of ζ are set at the time when the GWs are produced.

$$\begin{aligned} \Phi\left(\eta, \vec{k}\right) &= T_{\Phi}\left(\eta, k\right) \zeta\left(\vec{k}\right), \\ \Psi\left(\eta, \vec{k}\right) &= T_{\Psi}\left(\eta, k\right) \zeta\left(\vec{k}\right). \end{aligned} \tag{2.45}$$

Consequently, the scalar term can be written as

$$\Gamma_S\left(\eta_0, \vec{k}, \vec{n}\right) = \int_{\eta_{in}}^{\eta} d\eta' e^{ik\mu(\eta'-\eta_0)} \left[T_{\Phi}\left(\eta', k\right) \delta\left(\eta_{in} - \eta'\right) + \frac{\partial\left[T_{\Phi}\left(\eta', k\right) + T_{\Psi}\left(\eta', k\right)\right]}{\partial\eta'}\right] \zeta\left(\vec{k}\right) \tag{2.46}$$

using eq. (2.43) we find

$$\begin{aligned} \Gamma_{\ell m,S} &= 4\pi (-i)^{\ell} \int \frac{d^3k}{(2\pi)^3} e^{i\vec{k}\vec{x_0}} \left[T_{\Phi}\left(\eta_{in}, k\right) j_{\ell}\left(k\left(\eta_0 - \eta_{in}\right)\right) + \right. \\ &+ \left. \int_{\eta_{in}}^{\eta_0} d\eta' \frac{\partial\left[T_{\Phi}\left(\eta', k\right) + T_{\Psi}\left(\eta', k\right)\right]}{\partial\eta'} j_{\ell}\left(k\left(\eta_0 - \eta'\right)\right)\right] \zeta\left(\vec{k}\right) Y^*_{\ell m}\left(\vec{k}\right). \end{aligned} \tag{2.47}$$

As for CMB anisotropies, the first and the second term in eq. (2.47) represent a Sachs-Wolfe (SW) and integrated Sachs-Wolfe (ISW) effect respectively.

2.2.3 Tensor sourced term

Finally, the tensor term is

$$\Gamma_{\ell m,T} = \int d^2 n Y^*_{\ell m}(\vec{n}) \int \frac{d^3k}{(2\pi)^3} e^{i\vec{k}\vec{x}_0} \int_{\eta_{in}}^{\eta_0} d\eta' e^{ik\mu(\eta'-\eta_0)} \frac{1}{2} \frac{\partial \chi_{jk}\left(\eta', \vec{k}\right)}{\partial \eta'} n^j n^k. \tag{2.48}$$

We decompose the tensor modes in right and left-handed circular polarizations [65]

$$\chi_{ij} = \sum_{\lambda=\pm 2} e_{ij,\lambda}\left(\vec{k}\right) \chi(\eta, k)\, \xi_\lambda\left(\vec{k}\right). \tag{2.49}$$

In a circular basis the tensor polarization is defined as

$$e_{ij,\lambda} = \frac{e_{ij,+} + i\lambda e_{ij,\times}}{\sqrt{2}}. \tag{2.50}$$

When $\vec{k}$ is oriented along the z-axis,

$$e_{ij,+}\left(\vec{k}_z\right) = \begin{pmatrix} 1 & 0 & 0 \\ 0 & -1 & 0 \\ 0 & 0 & 0 \end{pmatrix} \quad e_{ij,\times}(\vec{k}_z) = \begin{pmatrix} 0 & 1 & 0 \\ 1 & 0 & 0 \\ 0 & 0 & 0 \end{pmatrix} \quad , \tag{2.51}$$

so that the only nonvanishing matrix elements are

$$\begin{aligned} \chi_{11}\left(\vec{k}_z\right) &= -\chi_{22} = \chi(\eta, k)\, \frac{\xi_{-2}\left(\vec{k}\right) + \xi_2\left(\vec{k}\right)}{2}, \\ \chi_{12}\left(\vec{k}_z\right) &= \chi_{21} = \chi(\eta, k)\, \frac{\xi_{-2}\left(\vec{k}\right) - \xi_2\left(\vec{k}\right)}{2i}. \end{aligned} \tag{2.52}$$

We decompose $\vec{n}$ the direction along the GW trajectory in a basis, in which $\vec{k}$ is oriented along the z-axis

$$\vec{n} = \left(\sqrt{1-\mu_{k,n}^2}\cos\phi_{k,n}, \sqrt{1-\mu_{k,n}^2}\sin\phi_{k,n}, \mu_{k,n}\right), \quad \text{where} \quad \mu_{k,n} = \cos\theta_{k,n}, \tag{2.53}$$

and so

$$
\begin{aligned}
- \quad & \frac{1}{2}\chi'_{jk}n^j n^k = -\frac{1-\mu_{k,n}^2}{2}\chi'(\eta,k)\left[\cos^2\phi_{k,n}\frac{\xi_{-2}\left(\vec{k}\right)+\xi_2\left(\vec{k}\right)}{2} - \sin^2\phi_{k,n}\frac{\xi_{-2}\left(\vec{k}\right)+\xi_2\left(\vec{k}\right)}{2} + \right. \\
+ \quad & \left. 2\cos\phi_{k,n}\sin\phi_{k,n}\frac{\xi_{-2}\left(\vec{k}\right)-\xi_2\left(\vec{k}\right)}{2}\right] \\
= \quad & -\frac{1-\mu_{k,n}^2}{2}\chi'(\eta,k)\left[\cos 2\phi_{k,n}\frac{\zeta_{-2}\left(\vec{k}\right)+\xi_2\left(\vec{k}\right)}{2} + \sin 2\phi_{k,n}\frac{\xi_{-2}\left(\vec{k}\right)-\xi_2\left(\vec{k}\right)}{2i}\right] \\
= \quad & -\frac{1-\mu_{k,n}^2}{4}\chi'(\eta,k)\left[e^{2\phi_{k,n}}\xi_2\left(\vec{k}\right)+e^{-2\phi_{k,n}}\xi_{-2}\left(\vec{k}\right)\right]. \qquad (2.54)
\end{aligned}
$$

The tensor term can be then rewritten as

$$
\Gamma_{\ell m,T} = \int \frac{d^3k}{(2\pi)^3}e^{i\vec{k}\vec{x}_0}\int d\Omega_n Y^*_{\ell m}(\Omega_n)\,\Gamma_T\left(\eta_0,\vec{k},\Omega_n\right), \qquad (2.55)
$$

with

$$
\Gamma_T\left(\eta_0,\vec{k},\Omega_n\right) = -\frac{1-\mu_{k,n}^2}{4}\left[e^{2\phi_{k,n}}\xi_2\left(\vec{k}\right)+e^{-2\phi_{k,n}}\xi_{-2}\left(\vec{k}\right)\right]\int_{\eta_{in}}^{\eta_0} d\eta e^{ik\mu_k(\eta-\eta_0)}\chi'(\eta,k). \qquad (2.56)
$$

This equation holds only if $\vec{k}$ is oriented along the z-axis. For a generic direction of $\vec{k}$ we introduce a rotation matrix

$$
S(\Omega_k) = \begin{pmatrix} \cos\theta_k\cos\phi_k & -\sin\phi_k & \sin\theta_k\cos\phi_k \\ \cos\theta_k\sin\phi_k & \cos\phi_k & \sin\theta_k\sin\phi_k \\ -\sin\theta_k & 0 & \cos\theta_k \end{pmatrix} \qquad (2.57)
$$

in terms of which

$$
\vec{k} = S(\Omega_k)\begin{pmatrix}0\\0\\1\end{pmatrix} \quad \begin{pmatrix}\cos\theta_k\cos\phi_k\\ \sin\theta_k\sin\phi_k\\ \cos\theta_k\end{pmatrix} = S(\Omega_k)\begin{pmatrix}\cos\theta_{k,n}\cos\phi_{k,n}\\ \sin\theta_{k,n}\sin\phi_{k,n}\\ \cos\theta_{k,n}\end{pmatrix} \qquad (2.58)
$$

Under this rotation

$$
Y^*_{\ell m}(\Omega_n) = \sum_{m'=-\ell}^{\ell} D^{\ell}_{mm'}(S(\Omega_k))Y^*_{\ell m'}(\Omega_{k,n}), \qquad (2.59)
$$

where the Wigner rotation matrix is given by

$$
D^{\ell}_{ms}(S(\Omega_k)) = \sqrt{\frac{4\pi}{2\ell+1}}(-1)^s Y^*_{\ell,-s}(\Omega_k), \qquad (2.60)
$$

in terms of the spin-weighted spherical harmonics

$$Y_{\ell m}^{*}\left(\theta,\phi\right)=\left(-1\right)^{m}\sqrt{\frac{2\ell+1}{4\pi}\frac{\left(\ell-m\right)!}{\left(\ell+m\right)!}}P_{\ell}^{m}\left(\cos\theta\right)e^{-im\phi}. \tag{2.61}$$

The associated Legendre polynomials are defined in terms of the Legendre polynomials as

$$\begin{aligned}P_{\ell}^{m}\left(\mu\right)&=\left(-1\right)^{m}\left(1-\mu^{2}\right)^{\frac{m}{2}}\frac{\mathrm{d}^{m}P_{\ell}\left(\mu\right)}{\mathrm{d}\mu^{m}},\\ P_{\ell}^{-|m|}\left(\mu\right)&=\left(-1\right)^{|m|}\frac{\left(\ell-|m|\right)!}{\left(\ell+|m|\right)!}P_{\ell}^{|m|}\left(\mu\right).\end{aligned} \tag{2.62}$$

We will also use the identity

$$\int\frac{d\mu}{2}P_{\ell}\left(\mu\right)e^{ik\mu(\eta-\eta_{0})}=\frac{1}{\left(-i\right)^{\ell}}j_{\ell}\left(k(\,\eta-\eta_{0}\,)\right). \tag{2.63}$$

With this relation

$$\Gamma_{\ell m,T}=\int\frac{d^{3}k}{\left(2\pi\right)^{3}}e^{i\vec{k}\vec{x_{0}}}\sum_{m=-\ell}^{\ell}D_{mm'}^{\ell}\left(S\left(\Omega_{k}\right)\right)\int d^{2}\Omega_{k,n}Y_{\ell m'}^{*}\left(\Omega_{k,n}\right)\Gamma_{T}\left(\eta_{0},\vec{k},\Omega_{k,n}\right). \tag{2.64}$$

The inner integral evaluates to

$$\begin{aligned}&\int d^{2}\Omega_{k,n}Y_{\ell m'}^{*}\left(\Omega_{k,n}\right)\Gamma_{T}\left(\eta_{0},\vec{k},\Omega_{k,n}\right)=\int d^{2}\Omega_{k,n}\sqrt{\frac{2\ell+1}{4\pi}\frac{\left(\ell-m'\right)!}{\left(\ell+m'\right)!}}P_{\ell}^{m'}\left(\mu_{k,n}\right)e^{-im'\phi_{k,n}}\\ &\left(-1\right)\frac{1-\mu_{k,n}^{2}}{4}\left[e^{2i\phi_{k,n}}\xi_{2}\left(\vec{k}\right)+e^{-2i\phi_{k,n}}\xi_{-2}\left(\vec{k}\right)\right]\int d\eta e^{ik\mu_{k}(\eta-\eta_{0})}\chi'\left(\eta,k\right)\\ &=-2\pi\int d\eta\chi'\left(\eta,k\right)\int d\mu_{k,n}\frac{1-\mu_{k,n}^{2}}{4}e^{ik\mu_{k}(\eta-\eta_{0})}\sqrt{\frac{2\ell+1}{4\pi}\frac{\left(\ell-2\right)!}{\left(\ell+2\right)!}}P_{\ell}^{2}\left(\mu_{k,n}\right)\\ &\left[\delta_{m',2}\xi_{2}\left(\vec{k}\right)+\delta_{m',-2}\xi_{-2}\left(\vec{k}\right)\right],\end{aligned} \tag{2.65}$$

and the integral over $\mu_{k,n}$ evaluates to

$$
\begin{aligned}
&\int \frac{d\mu_{k,n}}{4}\left(1-\mu_{k,n}^2\right)^2 e^{ik\mu_k(\eta-\eta_0)}\frac{\mathrm{d}^2 P_\ell\left(\mu_{k,n}\right)}{\mathrm{d}\mu_{k,n}^2}\\
=&\int \frac{d\mu_{k,n}}{4}e^{ik\mu_k(\eta-\eta_0)}\left(1-\mu_{k,n}^2\right)\left[2\mu_{k,n}\frac{\mathrm{d}P_\ell\left(\mu_{k,n}\right)}{\mathrm{d}\mu}-\ell(\ell+1)P_\ell\left(\mu_{k,n}\right)\right]\\
=&\int \frac{d\mu_{k,n}}{4}e^{ik\mu_k(\eta-\eta_0)}\left[\frac{2\mu_{k,n}\ell\left(\ell+1\right)}{ik\left(\eta-\eta_0\right)}P_\ell\left(\mu_{k,n}\right)+\frac{2\ell(\ell+1)}{k^2\left(\eta-\eta_0\right)^2}P_\ell\left(\mu_{k,n}\right)-\right.\\
-&\left.\frac{2\mu_{k,n}\ell\left(\ell+1\right)}{ik\left(\eta-\eta_0\right)}\ell\left(\ell+1\right)P_\ell\left(\mu_{k,n}\right)+\frac{2\ell\left(\ell+1\right)}{ik\left(\eta-\eta_0\right)}\left(1-\mu_{k,n}^2\right)\frac{\mathrm{d}P_\ell\left(\mu_{k,n}\right)}{\mathrm{d}\mu}\right]\\
=&\int \frac{d\mu_{k,n}}{4}e^{ik\mu_k(\eta-\eta_0)}\left[\frac{2\ell\left(\ell+1\right)}{k^2\left(\eta-\eta_0\right)^2}P_\ell\left(\mu_{k,n}\right)-\frac{2\ell^2\left(\ell+1\right)^2}{k^2\left(\eta-\eta_0\right)^2}P_\ell\left(\mu_{k,n}\right)\right]\\
=&-\frac{1}{2}\left(-1\right)^\ell\frac{j_\ell\left(k\left(\eta-\eta_0\right)\right)}{k^2\left(\eta-\eta_0\right)^2}\frac{(\ell+2)!}{(\ell-2)!},
\end{aligned}
\tag{2.66}
$$

then

$$
\begin{aligned}
&2\pi\int_{\eta_{in}}^{\eta_0}d\eta\chi'\left(\eta,k\right)\sqrt{\frac{2\ell+1}{4\pi}\frac{(\ell-2)!}{(\ell+2)!}}\left[\delta_{m',2}\xi_2\left(\vec{k}\right)+\delta_{m',-2}\xi_{-2}\left(\vec{k}\right)\right]\frac{1}{2}\left(-1\right)^\ell\frac{j_\ell\left(k\left(\eta-\eta_0\right)\right)}{k^2\left(\eta-\eta_0\right)^2}\frac{(\ell+2)!}{(\ell-2)!}=\\
&=\pi\left(-1\right)^\ell\int_{\eta_{in}}^{\eta_0}d\eta\chi'(\eta,k)\frac{j_\ell\left(k\left(\eta-\eta_0\right)\right)}{k^2\left(\eta-\eta_0\right)^2}\sqrt{\frac{2l+1}{4\pi}\frac{(\ell+2)!}{(\ell-2)!}}\left[\delta_{m',2}\xi_2\left(\vec{k}\right)+\delta_{m',-2}\xi_{-2}\left(\vec{k}\right)\right].
\end{aligned}
\tag{2.67}
$$

Inserting this into eq. (2.55), we find

$$
\begin{aligned}
\Gamma_{\ell m,T}=&\pi\left(-1\right)^\ell\int\frac{d^3k}{\left(2\pi\right)^3}e^{i\vec{k}\vec{x_0}}\int_{\eta_{in}}^{\eta_0}d\eta\chi'\left(\eta,k\right)\frac{j_\ell\left(k\left(\eta-\eta_0\right)\right)}{k^2\left(\eta-\eta_0\right)^2}\sqrt{\frac{2\ell+1}{4\pi}\frac{(\ell+2)!}{(\ell-2)!}}\\
&\sqrt{\frac{4\pi}{2\ell+1}}\left[Y_{\ell m,2}^*\left(\Omega_k\right)\xi_2\left(\vec{k}\right)+Y_{lm,-2}^*\xi_{-2}\left(\vec{k}\right)\right]\\
&=\pi\left(-1\right)^\ell\int\frac{d^3k}{\left(2\pi\right)^3}e^{i\vec{k}\vec{x_0}}\int d\eta\chi'\left(\eta,k\right)\frac{j_l\left(k\left(\eta-\eta_0\right)\right)}{k^2\left(\eta-\eta_0\right)^2}\sqrt{\frac{(\ell+2)!}{(\ell-2)!}}\\
&[Y_{\ell m,2}^*\left(\Omega_k\right)\xi_2\left(\vec{k}\right)+Y_{\ell m,-2}^*\xi_{-2}\left(\vec{k}\right)].
\end{aligned}
\tag{2.68}
$$

Finally, we obtain the tensor term

$$
\begin{aligned}
\Gamma_{\ell m,T}=&\pi\left(-i\right)^\ell\sqrt{\frac{(\ell+2)!}{(\ell-2)!}}\int\frac{d^3k}{\left(2\pi\right)^3}e^{i\vec{k}\vec{x_0}}\sum_{\lambda\pm2}Y_{\ell m,-\lambda}^*\left(\Omega_k\right)\xi_\lambda\left(\vec{k}\right)\\
&\int_{\eta_{in}}^{\eta_0}d\eta\chi'\left(\eta,k\right)\frac{j_\ell\left(k\left(\eta_0-\eta\right)\right)}{k^2\left(\eta_0-\eta\right)^2}.
\end{aligned}
\tag{2.69}
$$

2.3 Two-point angular correlators of the SGWB

We can now obtain a 2-point angular correlation function for the initial condition term $\Gamma\left(\eta_{in},\vec{k},q\right)$ and the stochastic variables determining the initial conditions of scalar and tensor perturbations $\zeta\left(\vec{k}\right)$ and $\xi_\lambda\left(\vec{k}\right)$,

$$\begin{aligned}\langle\Gamma\left(\eta_{in},\vec{k},q\right)\Gamma^*\left(\eta_{in},\vec{k'},q\right)\rangle &= \frac{2\pi^2}{k^3}P_I\left(q,k\right)\left(2\pi\right)^3\delta^{(3)}\left(\vec{k}-\vec{k'}\right),\\ \langle\zeta\left(\vec{k}\right)\zeta^*\left(\vec{k'}\right)\rangle &= \frac{2\pi^2}{k^3}P_\zeta\left(k\right)\left(2\pi\right)^3\delta^{(3)}\left(\vec{k}-\vec{k'}\right),\\ \langle\xi_\lambda\left(\vec{k}\right)\xi^*_\lambda\left(\vec{k'}\right)\rangle &= \frac{2\pi^2}{k^3}P_\lambda\delta_{\lambda\lambda'}\left(k\right)\left(2\pi\right)^3\delta^{(3)}\left(\vec{k}-\vec{k'}\right).\end{aligned} \tag{2.70}$$

From the CMB data, the stochastic variables $\zeta(\vec{k})$ and $\xi_\lambda(\vec{k})$ are nearly Gaussian [50]. We assume that this is the case also for the initial condition term.

Assuming statistical isotropy, we define the multipole coefficients as

$$\langle\Gamma_{\ell m}\Gamma^*_{\ell'm'}\rangle = \delta_{\ell\ell'}\delta_{mm'}\tilde{C}_\ell, \quad \text{where} \quad \tilde{C}_\ell = \tilde{C}_{\ell,I}\left(q\right)+\tilde{C}_{\ell,S}+\tilde{C}_{\ell,T}. \tag{2.71}$$

From eq. (2.44) we can write

$$\begin{aligned}\langle\Gamma_{\ell m,I}\left(q\right)\Gamma^*_{\ell'm',I}\left(q\right)\rangle = \left(4\pi\right)^2\left(-i\right)^{\ell-\ell'}\int\frac{d^3k}{\left(2\pi\right)^3}e^{i\vec{k}\vec{x_0}}\frac{d^3k'}{\left(2\pi\right)^3}e^{i\vec{k'}\vec{x_0}}Y^*_{\ell m}\left(\vec{k}\right)Y_{\ell'm'}\left(\vec{k'}\right)\\ \langle\Gamma_I\left(\eta_{in},\vec{k},q\right)\Gamma_I\left(\eta_{in},\vec{k'},q\right)\rangle j_\ell\left(k\left(\eta_0-\eta_{in}\right)\right)j_{\ell'}\left(k'\left(\eta_0-\eta_{in}\right)\right),\end{aligned} \tag{2.72}$$

and using the orthonormality condition for the spherical harmonics

$$\begin{aligned}\langle\Gamma_{\ell m,I}\left(q\right)\Gamma^*_{\ell'm',I}\left(q\right)\rangle &= \delta_{\ell\ell'}\delta_{mm'}\left(4\pi\right)^2\int\frac{k^2dk}{\left(2\pi\right)^3}\frac{2\pi^2}{k^3}P_I\left(q,k\right)\left(j_\ell\left(k\left(\eta_0-\eta_{in}\right)\right)\right)^2\\ &= \delta_{\ell\ell'}\delta_{mm'}4\pi\int\frac{dk}{k}P_I\left(q,k\right)\left(j_\ell\left(k\left(\eta_0-\eta_{in}\right)\right)\right)^2.\end{aligned} \tag{2.73}$$

In the end, we have

$$\tilde{C}_{\ell,I}(q) = 4\pi\int\frac{dk}{k}P_I\left(q,k\right)\left(j_\ell\left(k\left(\eta_0-\eta_{in}\right)\right)\right)^2. \tag{2.74}$$

Likewise, we can obtain the correlation functions for the scalar and tensor terms

$$\begin{aligned}
\tilde{C}_{\ell,S} &= 4\pi \int \frac{dk}{k} \left[T_\Phi(\eta_{in},k)\, j_\ell(k(\eta_0-\eta_{in})) + \right. \\
&+ \left. \int_{\eta_{in}}^{\eta_0} d\eta \frac{\partial \left[T_\Phi(\eta,k) + T_\Psi(\eta,k) \right]}{\partial \eta} j_\ell(k(\eta_0-\eta)) \right]^2 P_\zeta(k), \\
\tilde{C}_{\ell,T} &= \pi \int \frac{dk}{k} \left[\sqrt{\frac{(\ell+2)!}{(\ell-2)!}} \int_{\eta_{in}}^{\eta_0} d\eta \chi'(\eta,k) \frac{j_\ell(k(\eta_0-\eta))}{k^2(\eta_0-\eta)^2} \right]^2 \sum_{\lambda=\pm 2} P_\lambda(k). \quad (2.75)
\end{aligned}$$

This can be written in a more compact form as

$$\begin{aligned}
\tilde{C}_{\ell,I}(q) &= 4\pi \int \frac{dk}{k} \mathcal{T}^2_{\ell,I}(k,\eta_{in},\eta_0) P_I(q,k), \\
\tilde{C}_{\ell,S} &= 4\pi \int \frac{dk}{k} \mathcal{T}^2_{\ell,S}(k,\eta_{in},\eta_0) P_\zeta(k), \\
\tilde{C}_{\ell,T} &= 4\pi \int \frac{dk}{k} \mathcal{T}^2_{\ell,T}(k,\eta_{in},\eta_0) \sum_{\lambda=\pm 2} P_\lambda(k).
\end{aligned} \quad (2.76)$$

where $\mathcal{T}_{\ell,I}$, $\mathcal{T}_{\ell,S}$ and $\mathcal{T}_{\ell,T}$ are the transfer functions defined as

$$\begin{aligned}
\mathcal{T}_{\ell,I}(k,\eta_{in},\eta_0) &= T_I(\eta_{in},k)\, j_\ell(k(\eta_0-\eta_{in})), \\
\mathcal{T}_{\ell,S}(k,\eta_{in},\eta_0) &= T_\Phi(\eta_{in},k)\, j_\ell(k(\eta_0-\eta_{in})) + \int_{\eta_{in}}^{\eta_0} d\eta \frac{\partial \left[T_\Phi(\eta,k) + T_\Psi(\eta,k) \right]}{\partial \eta} j_l(k(\eta_0-\eta)), \\
\mathcal{T}_{\ell,T}(k,\eta_{in},\eta_0) &= \frac{1}{4} \sqrt{\frac{(\ell+2)!}{(\ell-2)!}} \int_{\eta_{in}}^{\eta_0} d\eta \chi'(\eta,k) \frac{j_\ell(k(\eta_0-\eta))}{k^2(\eta_0-\eta)^2}.
\end{aligned} \quad (2.77)$$

Chapter 3

Initial conditions

3.1 Einstein equations

To compute the angular power spectrum of the SGWB we need to know the initial conditions for the GW energy density perturbation δ_{GW} and the evolution of gravitational potentials Φ and Ψ. For this, we need the Einstein equations

$$G_{\mu\nu} = 8\pi G T_{\mu\nu}\,. \tag{3.1}$$

Since scalar, vector, and tensor perturbations are independent at first order, we can consider the Einstein equations for each mode independently.

The line element in the Poisson gauge at first order for scalar perturbations is [26]

$$ds^2 = a^2(\eta)\left[-(1+2\Phi)\,d\eta^2 + (1-2\Psi)\,\delta_{ij}dx^i dx^j\right]. \tag{3.2}$$

The Einstein tensor is defined as

$$G_{\mu\nu} \equiv R_{\mu\nu} - \frac{1}{2}g_{\mu\nu}R. \tag{3.3}$$

The Christoffel symbols up to first order are given by

$$\begin{aligned}
\Gamma^0_{00} &= \mathcal{H} + \Phi' \\
\Gamma^0_{0i} &= \partial_i\Phi \\
\Gamma^0_{ij} &= \left[\mathcal{H}(1-2\Psi-2\Phi) - \Psi'\right]\delta_{ij} \\
\Gamma^i_{00} &= \partial^i\Phi \\
\Gamma^i_{j0} &= \left[\mathcal{H} - \Psi'\right]\delta^i_j \\
\Gamma^i_{jk} &= \partial^i\Psi\delta_{jk} - \partial_j\Psi\delta^i_k - -\partial_k\Psi\delta^i_j.
\end{aligned} \tag{3.4}$$

From this, we can derive the Ricci tensor,

$$\begin{aligned}
\delta R_{00} &= \nabla^2\Phi + 3\Psi'' + 3\frac{a'}{a}\Psi + 3\frac{a'}{a}\Phi \\
\delta R_{0i} &= 2\partial_i\Psi + 2\frac{a'}{a}\partial_i\Phi \\
\delta R_{ij} &= \left[-\frac{a'}{a}\Phi' - 5\frac{a'}{a}\Psi' + 2\frac{a''}{a}\Phi - 2\left(\frac{a'}{a}\right)^2\Phi - 2\frac{a''}{a}\Psi\right. \\
&- \left. 2\left(\frac{a'}{a}\right)^2\Psi - \Psi'' + \nabla^2\Psi\delta_{ij} + \partial_i\partial_j\Psi - \partial_i\partial_j\Phi\right]
\end{aligned} \tag{3.5}$$

Finally, we can evaluate the Einstein tensor

$$\begin{aligned}
G_{00} &= \frac{1}{a^2}\left[\mathcal{H}^2\left(6\Phi - 3\right) + 6\Psi' - 2\nabla^2\Psi\right] \\
G_i^0 &= -\frac{2}{a^2}\left[\mathcal{H}\partial_i\Phi + \partial_i\Psi'\right] \\
G_j^i &= \frac{1}{a^2}\left[\left[-2\frac{a''}{a}\left(1 - 2\Phi\right) + \mathcal{H}^2\left(1 - 2\Phi\right) + 2\mathcal{H}\Phi' + 4\mathcal{H}\Phi' + 2\Phi''\right.\right. \\
&- \left.\left.\nabla^2\Psi + \nabla^2\Phi\right]\delta_j^i + \partial^i\partial_j\left(\Psi - \Phi\right)\right].
\end{aligned} \tag{3.6}$$

To complete our derivation of the Einstein equation we need to compute the stress-energy tensor at first order. The (0,0) component of stress-energy tensor is defined as the energy density of all particle species in the universe $T_0^0 = \rho$. We can write

$$T_0^0 = -\sum_i g_i \int \frac{d^3p}{(2\pi)^3} E_i f_i = -\sum_i \frac{g_i}{a^3}\int \frac{d^3q}{(2\pi)^3} E_i f_i. \tag{3.7}$$

where g_i is the number of effective degrees of freedom, E_i is the energy of a particle and f_i is the distribution function of a particle species. In order to obtain the stress-energy tensor at first order, we must consider the distribution function at first order, so

$$T_0^0 = -\sum_i \frac{g_i}{a^3}\int \frac{d^3q}{(2\pi)^3} E_i\left[f_i^{(0)} + \delta f_i\right] = -\sum_i \left[\rho_i^0 + \frac{g_i}{a^3}\int \frac{d^3q}{(2\pi)^3} E_i\delta f_i\right] \tag{3.8}$$

The various particle species that contribute to the energy density of the universe include photons, neutrinos, and dark matter. The GWs in general should also be included, but their relative contribution to the total energy density of the universe is negligible. We can write [26]

$$\begin{aligned}
f_\gamma &= f_\gamma^{(0)} - q\frac{\mathrm{d}f_\gamma^{(0)}}{\mathrm{d}q}\Theta, \\
f_\nu &= f_\nu^{(0)} - q^{(0)}\frac{\mathrm{d}f_\nu}{\mathrm{d}q}N, \\
\rho_m &= \rho_m^{(0)}\left(1 + \delta_m\right),
\end{aligned} \tag{3.9}$$

where Θ, N denote the perturbation in the distribution function for photons f_γ and neutrinos f_γ respectively and δ_m is the matter energy density perturbation. Inserting these definitions in eq. (3.8) we get

$$\begin{aligned} T_{00} &= -\left[\rho_\gamma^{(0)} + \frac{g_i}{a^3}\int \frac{d^3q}{(2\pi)^3} q \frac{\mathrm{d}f_\gamma}{\mathrm{d}q}\theta\right] - \left[\rho_\nu^{(0)} + \frac{g_i}{a^3}\int \frac{d^3q}{(2\pi)^3} q \frac{\mathrm{d}f_\nu}{\mathrm{d}q} N\right] + \rho_m^{(0)}\left(1+\delta_m\right) \\ &= -\rho_\gamma^{(0)}\left[1+4\theta_0\right] - \rho_\nu^{(0)}\left[1+4N_0\right] + \rho_m^{(0)}\left(1+\delta_m\right), \end{aligned} \tag{3.10}$$

where θ_0 ans N_0 are the monopole contributions of the distribution function

$$\theta_0 \equiv \frac{1}{4\pi}\int d\Omega\, \theta. \tag{3.11}$$

Equating G_0^0 and $8\pi G T_0^0$, we obtain the (0,0) Einstein equation

$$\nabla^2\Psi - 3\mathcal{H}\left(\Psi' + \mathcal{H}\Phi\right) = -4\pi G a^2\left[\rho_m^{(0)}\delta_m + \rho_\gamma^{(0)}\Theta_{\gamma,0} + \rho_\nu^{(0)}\Theta_{\nu,0}\right]. \tag{3.12}$$

Since we have only two unknown variables Φ and Ψ, we consider only the traceless longitudinal part of the (i,j) Einstein equation. To separate the traceless longitudinal part, we apply the projection operator $\hat{k}^j\hat{k}_i - \frac{1}{3}\delta_{ij}$ to the Einstein tensor G_j^i in Fourier space

$$\left(\hat{k}^j\hat{k}_i - \frac{1}{3}\delta_{ij}\right) G_j^i = \frac{2k^2}{3a^2}\left(\Psi - \Phi\right). \tag{3.13}$$

Analogously, for the stress-energy tensor T_j^i we have

$$\begin{aligned} \left(\hat{k}^j\hat{k}_i - \frac{1}{3}\delta_{ij}\right) T_j^i &= \sum_i \frac{g_i}{a^4}\int \frac{d^3q}{(2\pi)^3} q \left(\hat{k}^j\hat{k}_i - \frac{1}{3}\delta_{ij}\right) n^i n_j f_i \\ &= \sum_i \frac{g_i}{a^4}\int \frac{d^3q}{(2\pi)^3} q\left(\mu^2 - 1/3\right) f_i = -\frac{8}{3}\left(\rho_\gamma^{(0)}\theta_2 + \rho_\nu^{(0)} N_2\right). \end{aligned} \tag{3.14}$$

The integral over μ for $f_i^{(0)}$ is null, because $f_i^{(0)}$ is the isotropic part of the distribution function. The quadrupole is defined as

$$f_2 \equiv -\int \frac{d\mu}{2} P_2\left(\mu\right) f. \tag{3.15}$$

Therefore the second Einstein equation is

$$k^2\left(\Phi - \Psi\right) = -32\pi G a^2\left(\rho_\gamma^{(0)}\theta_2 + \rho_\nu^{(0)} N_2\right). \tag{3.16}$$

Non-relativistic particles are completely characterized by energy density and velocity, therefore they do not contribute to a quadrupole term. The two gravitational potentials are equal if the photons and neutrinos quadrupole moment is negligible. The photon

quadrupole moment adds little to the sum because it is very small when the energy density of the photons is appreciable, that is during the radiation era. Therefore only neutrinos contribute to a significant quadrupole moment in the early universe. The (0, i) component of the Einstein tensor in Fourier space is

$$G_i^0 = -\frac{2ik_i}{a^2}\left[\mathcal{H}\Phi + \Psi'\right]. \tag{3.17}$$

The (0, i) component of stress-energy tensor is

$$\begin{aligned} T_i^0 &= \sum_i \frac{1}{a^4}\int \frac{d^3q}{(2\pi)^3} q\delta_{ij}n^j f_j \\ &= \rho_m^{(0)} v^i \delta_{ij} + 4\rho_r \int \frac{d\mu}{2} P_1(\mu)\,\theta_r. \end{aligned} \tag{3.18}$$

We obtain then the (0, i) Einstein equation projected along k^i

$$\mathcal{H}\Phi + \Psi' = \rho_m^{(0)} v_m + 4\rho_\gamma^{(0)}\theta_{\gamma,1} + 4\rho_\nu^{(0)}\theta_{\nu,1}. \tag{3.19}$$

We can also write the first Einstein equation in Fourier space as

$$-k^2\Psi - 3\mathcal{H}\left(\Psi' + \mathcal{H}\Phi\right) = -4\pi G a^2\left[\rho_m^{(0)}\delta_m + \rho_\gamma^{(0)}\Theta_{\gamma,0} + \rho_\nu^{(0)}\Theta_{\nu,0}\right]. \tag{3.20}$$

Combining of (0,0) and (0, i) Einstein equations leads to

$$\Phi = -\frac{4\pi G a^2}{k^2}\left[\rho_m^{(0)}\delta_m + \rho_\gamma^{(0)}\Theta_{\gamma,0} + \rho_\nu^{(0)}\Theta_{\nu,0} + \frac{3\mathcal{H}}{k}\left[\rho_m^{(0)} v_m + 4\rho_\gamma^{(0)}\theta_{\gamma,1} + 4\rho_\nu^{(0)}\theta_{\nu,1}\right]\right]. \tag{3.21}$$

3.2 Einstein and Boltzmann equation at early times

The Boltzmann equations for the photons and neutrinos are [26]

$$\begin{aligned} &\Theta' + ik\mu\Theta = \Psi' - ik\mu\Phi - \tau'\left(\theta_0 - \theta + \mu v_b - \frac{1}{2}P_2(\mu)\,\theta_2\right) \\ &N' + ik\mu N = \Psi' - ik\mu\Phi. \end{aligned} \tag{3.22}$$

where τ is the optical depth defined as

$$\tau(\eta) \equiv \int d\eta' n_e \sigma_T a, \tag{3.23}$$

where n_e is the electron number density and σ_T is the cross section for Compton scattering. At early times the optical depth is large due to the scattering of photons and electrons, while it is very small at late times since the free electron number density

is very small. The equation for neutrinos is identical to the photons except that for neutrinos there is no scattering term since neutrinos interact very weakly.

At early times $k\eta \ll 1$, we can neglect the terms multiplied by k. The higher multipoles will be much smaller than the monopole term θ_0. The Boltzmann equations for the photons and neutrinos then read

$$\begin{aligned} \Theta_0' &= \Psi' \,, \\ N_0' &= \Psi' \,. \end{aligned} \tag{3.24}$$

In the Einstein equation at early times the term, which contains a factor of k^2 can be neglected. Also, the matter contribution is negligible at early times, when the radiation dominates. Thus, we get

$$3\mathcal{H}\left(\Psi' + \mathcal{H}\Phi\right) = -4\pi G a^2 \left[\rho_\gamma \Theta_{\gamma,0} + \rho_\nu \Theta_{\nu,0}\right] . \tag{3.25}$$

We can simplify the equation by introducing the ratio of neutrino energy density to the total radiation energy density

$$f_\nu = \frac{\rho_\nu}{\rho_\gamma + \rho_\nu}, \tag{3.26}$$

then the equation reads

$$3H\left(\Psi' + \mathcal{H}\Phi\right) = -4\pi G a^2 \rho_r \left[\left(1 - f_\nu\right)\Theta_0 + f_\nu N_0\right] . \tag{3.27}$$

In the radiation dominated universe $a \propto \eta$, so $a'/a \propto 1/\eta$, thus

$$\begin{aligned} \frac{\Phi'}{\eta} - \frac{\Psi}{\eta^2} &= \frac{-4\pi G \rho_r a^2}{3} \left[\left(1 - f_\nu\right)\Theta_0 + f_\nu N_0\right] \\ &= \frac{2}{\eta} \left[\left(1 - f_\nu\right)\Theta_0 + f_\nu N_0\right] \end{aligned} \tag{3.28}$$

then

$$\Phi'\eta - \Psi = 2\left[\left(1 - f_\nu\right)\Theta_0 + f_\nu N_0\right] . \tag{3.29}$$

By differentiating both sides of the equation and using eq. (3.24), we have

$$\Phi''\eta + \Phi' - \Psi' = -2\Phi' \tag{3.30}$$

If we neglect the quadrupole moments in eq. (3.16), then $\Phi = \Psi$. Under this approximation we have

$$\Phi'\eta + 4\Phi' = 0 \tag{3.31}$$

Setting $\Phi = \eta^p$, we get the algebraic equation

$$p\left(p - 1\right) + 4p = 0, \tag{3.32}$$

which has two solutions $p = 0$, the growing mode, which is constant in time, and $p = -3$, the decaying mode, which quickly dies out. We are interested in the growing mode, so eq. (3.29) becomes

$$\Phi = -2\left[(1 - f_\nu)\,\Theta_0 + f_\nu N_0\right] \tag{3.33}$$

Since in the early universe the perturbations tend to not distinguish between photons and neutrinos [26]

$$\Theta_0 = N_0, \tag{3.34}$$

which leads to

$$\Phi = -2\Theta_0 = -2N_0. \tag{3.35}$$

Since for the photons $\rho_\gamma \propto T^4$

$$\delta_\gamma = \frac{\delta\rho_\gamma}{\rho_\gamma} = \frac{4\delta T}{T} = 4\Theta_0. \tag{3.36}$$

The primordial density perturbations can be divided into adiabatic perturbations and isocurvature ones. Adiabatic perturbations are characterized by vanishing entropy perturbation. The gauge-invariant entropy perturbation for the two-particle species i and j is defined as

$$S_{ij} = \frac{\delta\rho_i}{1 + w_i} - \frac{\delta\rho_j}{1 + w_j}. \tag{3.37}$$

For adiabatic perturbations, $S_{ij} = 0$ and consequently the perturbations in all components are proportional and related by

$$\delta_m = \frac{3}{4}\delta_\gamma = \frac{3}{4}\delta_\nu = \frac{3}{4}\delta_{\mathrm{GW}}. \tag{3.38}$$

We have found the relation for the photon energy density perturbation from the Einstein equation, therefore using the fact that for adiabatic perturbations δ_{GW} follows δ_γ, we can write

$$\delta_{\mathrm{GW}} = \delta_\gamma = -2\Phi. \tag{3.39}$$

The initial condition term can be expressed in terms of the initial energy density perturbation as [23]

$$\Gamma_I\left(\eta_{in}, k\right) = \frac{\delta_{\mathrm{GW}}\left(\eta_{in}, k\right)}{4 - n_T}. \tag{3.40}$$

So using eq. (3.39), we obtain

$$\Gamma_I\left(\eta_{in}, k\right) = \frac{-2\Phi\left(\eta_{in}, k\right)}{4 - n_T}. \tag{3.41}$$

In the case of isocurvature perturbations $S_{ij} \neq 0$. The GW energy density perturbation on large scales during the radiation-dominated epoch can be written as [28]

$$\delta_{\rm GW} = \delta_{\rm GW}^{prim} + 4\Phi_{RD}, \tag{3.42}$$

where Φ_{RD} is the gravitational potential, which is related to the curvature perturbation during the radiation-dominated epoch through

$$\zeta_{RD} = -\frac{3}{2}\Phi_{RD}. \tag{3.43}$$

We can decompose the curvature perturbation during the radiation-dominated epoch as

$$\zeta_{RD} = (1 - f_\nu - f_{\rm GW})\zeta_\gamma + f_\nu\zeta_\nu + f_{\rm GW}\zeta_{\rm GW} = \zeta_\gamma + \frac{1}{3}f_{\rm GW}S_{\rm GW}, \tag{3.44}$$

where S_{GW} is the entropy perturbation defined as

$$S_{\rm GW} = 3\left(\zeta_{\rm GW} - \zeta_\gamma\right). \tag{3.45}$$

Consequently, the GW energy density perturbation is

$$\delta_{\rm GW} = -\frac{4}{3}\zeta_{RD} + \frac{4}{3}\left(1 - f_{\rm GW}\right)S_{GW}. \tag{3.46}$$

Chapter 4

Results

To compute the angular power spectrum of the SGWB we will use using the Cosmic Linear Anisotropy Solving System (CLASS) [29]. CLASS is the Boltzmann code that is written in C, but organized in a few modules that reproduce the C++ classes. It simulates the dynamics of linear perturbations and computes CMB and large-scale structure observables, such as the CMB angular power spectrum.

We want to evaluate the angular power spectrum of the SGWB

$$\begin{aligned}\tilde{C}_\ell(q) &= 4\pi \int \frac{dk}{k} \left[\mathcal{T}^2_{\ell,I}(k,\eta_{in},\eta_0)\, P_I(k,q) + \mathcal{T}^2_{\ell,S}(k,\eta_{in},\eta_0)\, P_\zeta(k)\right. \\ &+ \left. \mathcal{T}^2_{\ell,T}(k,\eta_{in},\eta_0) \sum_{\lambda=\pm 2} P_\lambda(k)\right], \end{aligned} \tag{4.1}$$

therefore we have to modify CLASS for the SGWB. For the CMB the angular power spectrum can be written as [26]

$$C_\ell = 4\pi \int \frac{dk}{k} \theta^2_\ell(\eta_0,k)\, P(k), \tag{4.2}$$

where $P(k)$ is the primordial power spectrum and $\theta_\ell(k)$ is the transfer function, as for SGWB, for scalar ($\alpha = 0$) and tensor ($\alpha = \pm 2$) modes

$$\begin{aligned}\theta^{(0)}_\ell(k) &= \int d\eta S^{(0)}_T(\eta,k)\, j_\ell(k(\eta_0-\eta)), \\ \theta^{(\alpha)}_\ell(k) &= \int d\eta S^{(\alpha)}_T(\eta,k)\, \frac{1}{4}\sqrt{\frac{(l+2)!}{(l-2)!}}\, \frac{j_\ell(k(\eta_0-\eta))}{k^2(\eta_0-\eta')^2}, \end{aligned} \tag{4.3}$$

where $S^{(0)}_T$ and $S^{(\alpha)}_T$ are the source functions given by

$$\begin{aligned} S^{(0)}_T(\eta,k) &= g\left(\frac{\delta_g}{4}+\Phi\right) + \left(gK^{-2}\theta_b\right)' + e^{-K}\left(\Phi'+\Psi'\right), \\ S^{(\alpha)}_T(\eta,k) &= -e^{-K}\chi' \end{aligned} \tag{4.4}$$

where $g = -K'e^{-K}$ is the visibility function and K is the optical depth. Since gravitons decouple at very early time, the collision term in the Boltzmann equation is zero, therefore we have to modify the source function by setting $g = 1$, $e^{-K} = 1$. Then the source function for gravitons reads

$$\begin{aligned} S_T^{(0)}(\eta, k) &= \Gamma(\eta_{in}, k) + \Phi(\eta_{in}, k) + \Phi'(\eta, k) + \Psi'(\eta, k), \\ S_T^{(\alpha)}(\eta, k) &= \chi'. \end{aligned} \tag{4.5}$$

The initial integration time η_{in} of the source function for the CMB corresponds to the recombination $T \simeq 0.3\,eV$. The GWs decouple at the Plank energy scale, thus we also have to change the initial time of integration. We set η_{in} at the time of neutrino decoupling $T \simeq 1\,\mathrm{MeV}$, which is early enough to mimic the effect associated with the propagation of GWs.

It is possible to specify the initial conditions for the energy density perturbation in CLASS. In general, the angular power spectrum can be written as the sum of contributions from adiabatic and isocurvature modes

$$\tilde{C}_\ell(q) = 4\pi \int \frac{dk}{k} \left[P_{ad}(q, k)\, \mathcal{T}_{ad}^2(\eta_0, k) + P_{\mathrm{iso}}(q, k)\, \mathcal{T}_{iso}^2(\eta_0, k) \right]. \tag{4.6}$$

Whether the perturbations are adiabatic or isocurvature would modify the initial conditions term $\Gamma(\eta_{in}, k)$ and the evolution of gravitational potentials $\Phi(\eta, k)$ and $\Psi(\eta, k)$.

4.1 Angular power spectrum of SGWB for adiabatic initial conditions

The initial condition term in case of adiabatic perturbations from eq. (3.41) is

$$\Gamma_I(\eta_{in}, k) = \frac{-2\Phi(\eta_{in}, k)}{4 - n_T}. \tag{4.7}$$

We consider the scale-invariant power spectrum, $n_T = 0$, so

$$\Gamma(\eta_{in}, k) = -\frac{1}{2}\Phi(\eta_{in}, k). \tag{4.8}$$

If we can disregard the tensor term contribution to the anisotropy of SGWB, which does not change the spectrum significantly, then we can write the adiabatic primordial power spectrum as

$$P_{ad}(k) = P_\zeta(k), \tag{4.9}$$

and the tranfer function $\mathcal{T}_{ad}(q, k)$ is given by

$$\mathcal{T}_{ad}(\eta_0, k) = \frac{1}{2} T_\Phi(\eta_{in}, k)\, j_\ell(k(\eta_0 - \eta_{in})) + \int_{\eta_{in}}^{\eta} d\eta \frac{\partial \left[T_\Phi(\eta, k) + T_\Psi(\eta, k) \right]}{\partial \eta} j_\ell(k(\eta_0 - \eta)). \tag{4.10}$$

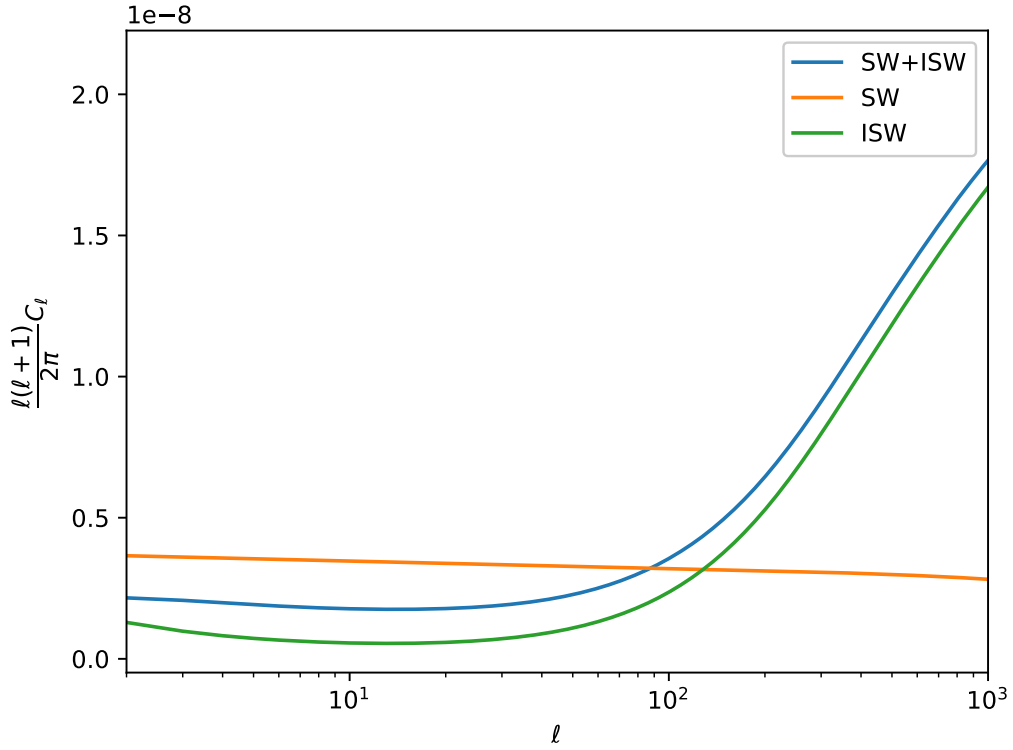

Figure 4.1: SW, ISW and total contribution to the angular power spectrum of the GW energy density perturbation for adiabatic initial conditions with the tensor spectral tilt $n_T = 0$, the scalar spectral tilt $n_S = 0.96$ and the primordial amplitude $A_S = 2.101 \cdot 10^{-9}$.

In Fig. 4.1 we report the SW, ISW and total contribution to the angular power spectrum of the GW energy density perturbation with the tensor spectral tilt $n_T = 0$ and the scalar spectral tilt $n_S = 0.96$ [66] and the primordial amplitude $A_S = 2.101 \cdot 10^{-9}$ [67]. The SW and the ISW contributions are depicted separately to demonstrate that on large scales, that is at lower ℓ, the SW effect provides the dominant contribution to the anisotropy of the SGWB and the spectrum is almost scale-invariant $l\,(l+1)\,C_l \propto const$, analogously to CMB anisotropies. The ISW effect starts to be larger on smaller scales, that is at higher ℓ.

4.2 Angular power spectrum of SGWB for isocurvature initial conditions

The initial condition term in the case of scale-invariant tensor power spectrum can be written as (3.40)

$$\Gamma_I(\eta_{in}, k) = 4\delta_{\rm GW}(\eta_{in}, k). \tag{4.11}$$

We consider that the source of isocurvature perturbation is cold dark matter. From [68, 69] the primordial GW energy density perturbation in the case of CDM isocurvature perturbations can be approximately expressed in terms of gravitational potential Φ as

$$\delta_{\rm GW}(\eta_{in}, k) \simeq -\frac{8}{3}\frac{2(15+2R_\nu)}{4R_\nu - 15}\Phi(\eta_{in}, k), \tag{4.12}$$

where R_ν is the fractional contribution of neutrinos to the total density at early times defined as

$$R_\nu = \frac{R}{1+R}, \tag{4.13}$$

where

$$R = \frac{7}{8}N_\nu\left(\frac{4}{11}\right)^{\frac{4}{3}}. \tag{4.14}$$

Assuming that the number of neutrino species $N_\nu = 3$, then $R_\nu = 0.4$. The initial condition term then is

$$\Gamma_I(\eta_{in}, k) \simeq -\frac{4}{3}\frac{15+2R_\nu}{4R_\nu - 15}\Phi(\eta_{in}, k). \tag{4.15}$$

As well as for adiabatic modes we disregard the tensor term contribution to the anisotropy of the SGWB. We introduce the isocurvature fraction defined as [66]

$$\beta_{iso}(k) = \frac{P_{iso}(k)}{P_{ad}(k) + P_{iso}(k)}. \tag{4.16}$$

The constrains on this parameter for the CDM isocurvature perturbations are given by the CMB data. It takes different values depending on the scalar spectral tilt and the correlation of the CDM isocurvature and adiabatic modes. We assume that isocurature and adiabtic modes are arbitrarily correlated and the scalar spectral tilt $n_S = 0.96$ is equal for both CDM isocurvature and adiabatic modes. This is a scenario predicted by some curvaton models. The isocurvature fraction is then [66]

$$\beta_{iso} = 0.039. \tag{4.17}$$

The primordial power spectrum for CDM isocurvature initial conditions can be written in terms of isocurvature fraction and the primordial adiabatic power spectrum as

$$P_{\rm iso}(k) = \frac{\beta_{iso}}{1-\beta_{iso}}P_\zeta(k). \tag{4.18}$$

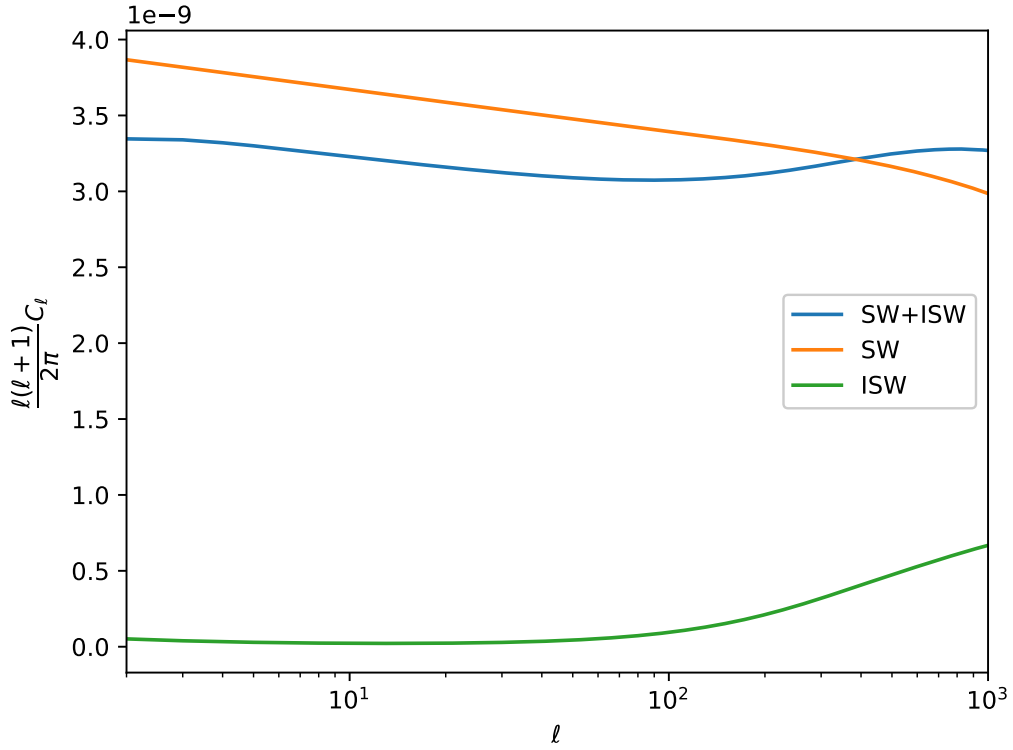

Figure 4.2: SW, ISW and total contribution to the angular power spectrum of the GW energy density perturbation for CDM isocurvature initial conditions with the tensor spectral tilt $n_T = 0$, the scalar spectral tilt $n_S = 0.96$, the primordial amplitude $A_S = 2.101 \cdot 10^{-9}$ and the isocurvature fraction $\beta_{iso} = 0.039$.

In general, the isocurvature modes are sourced by the second scalar field present during inflation or phase transition. If it decays shortly after the end of inflation or phase transition, then the isocurvature perturbations would not significantly affect the transfer function, then it can be written similarly to the adiabatic case taking into account the modified initial condition term

$$\begin{aligned} \mathcal{T}_{iso}\left(\eta_0, k\right) = \frac{1}{3}\,\frac{4R_\nu - 105}{R_\nu - 15} T_\Phi\left(\eta_{in}, k\right) j_l\left(k(\,\eta_0 - \eta_{in}\,)\right) \\ + \int_{\eta_{in}}^{\eta} d\eta \frac{\partial\left[T_\Phi\left(\eta, k\right) + T_\Psi\left(\eta, k\right)\right]}{\partial\eta} j_l\left(k\left(\eta_0 - \eta\right)\right). \end{aligned} \tag{4.19}$$

In Fig. 4.2 we report the SW, ISW and total contribution to the angular power spectrum of the GW energy density perturbation for CDM isocurvature initial conditions with the tensor spectral tilt $n_T = 0$, the scalar spectral tilt $n_S = 0.96$ [66] , the primordial amplitude $A_S = 2.101 \cdot 10^{-9}$ [67] and the isocurvature fraction $\beta_{iso} = 0.039$.

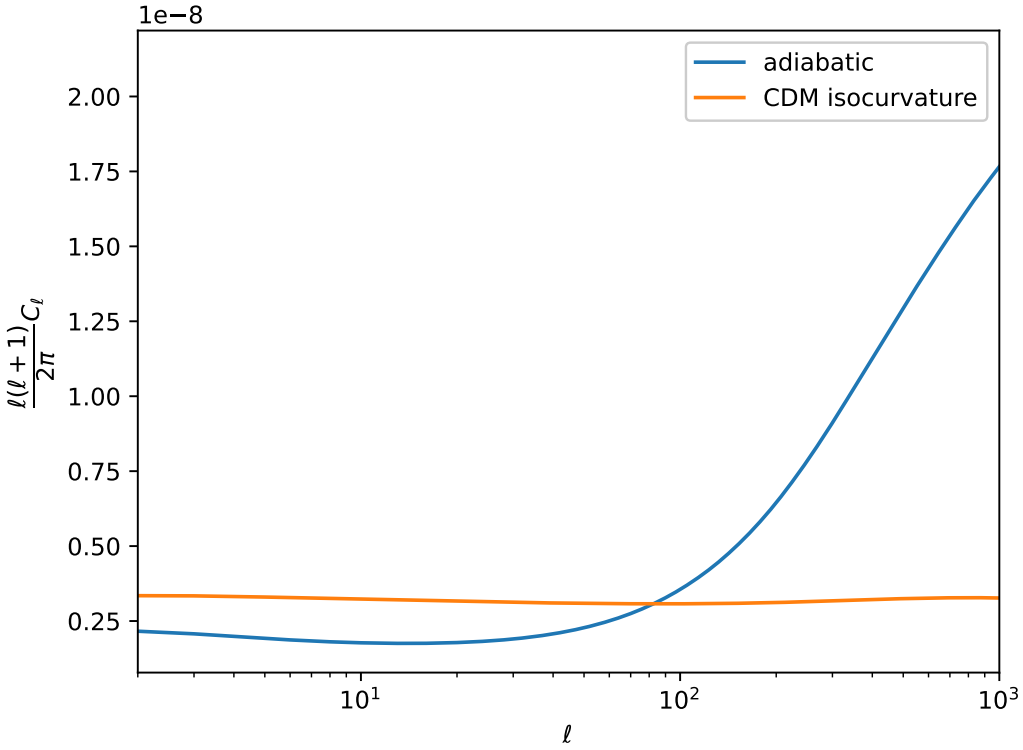

Figure 4.3: Total angular power spectrum of the GW energy density perturbation for CDM isocurvature and adiabatic initial conditions.

The initial condition term in the case of CDM isocurvature perturbations is larger compared to the adiabatic case due to the modified initial condition term in eq. (4.19). However, the SW effect for both isocurvature and adiabatic perturbations is almost identical, since the isocurvature primordial power spectrum is smaller than the adiabatic one (4.18), which compensates the prefactor in the initial condition term. We can write the ratio of the SW effect in both cases

$$\frac{C_\ell^{SW,iso}}{C_\ell^{SW,ad}} \simeq \frac{\beta_{iso}}{1-\beta_{iso}} \frac{\left(\Gamma_I^{iso} + \Phi\left(\eta_{in}\right)\right)^2}{\left(\Gamma_I^{ad} + \Phi\left(\eta_{in}\right)\right)^2} \simeq \frac{\beta_{iso}}{1-\beta_{iso}} \left(\frac{1}{6}\,\frac{4R_\nu - 105}{R_\nu - 15}\right)^2 \approx 1.05. \tag{4.20}$$

Furthermore, in the isocurvature case, we do not observe the growth of the ISW effect on smaller scales as for adiabatic initial conditions due to the fact that the ratio between the SW and ISW effect is far greater compared to the adiabatic case.

In Fig. 4.3 we show the comparison between the total angular power spectrum of the GW energy density perturbation for adiabatic and CDM isocurvature initial conditions.

On large scales, the total power spectrum for CDM isocurvature perturbations is larger than the adiabatic one by the fraction

$$\frac{C_\ell^{iso}}{C_\ell^{ad}} \simeq 1.67. \tag{4.21}$$

This is due to the late ISW effect, which is important on large scales and has a negative relative sign with respect to the SW effect. The late ISW effect for the adiabatic perturbations is much larger than for isocurvature ones since the isocurvature primordial power spectrum is far smaller than the adiabatic one (4.18).

These particular traits of the angular power spectrum for the CDM isocurvature initial condition compared with the adiabatic case may allow to distinguish among the GW sources, that induce either isocurvature or adiabatic perturbations.

Chapter 5

Conclusions

In this thesis, we have studied the effect of different cosmological sources on the SGWB anisotropies. We considered how the presence of isocurvature perturbations in the early universe would impact the angular anisotropy of the SGWB and we compared it with the adiabatic sources of GWs.

In Chapter 1 we have reviewed several mechanisms in the early universe that could be source GWs, are inflation, phase transitions, and cosmic strings. We studied the SGWB from the quantum fluctuations of the metric during inflation, but also from the multi-field models of inflation. This includes the axion inflation model, where the inflaton field is coupled to a gauge field, which similarly to the vacuum fluctuations produces adiabatic perturbations. We have also considered models which lead to the isocurvature perturbations, like the inclusion of an extra scalar spectator field and the curvaton scenario. In this latter mechanism, the final curvature perturbations are generated by an initial isocurvature perturbation of the curvaton. Then we described the production of GWs during a first-order phase transition due to the collision of bubble walls, sound waves, and magneto-hydrodynamic turbulence. We have also considered the GWs produced by a network of cosmic string loops. We presented the average GW energy density for these mechanisms of GW production in the early universe.

In Chapter 2 in order to study the anisotropy of the SGWB we solved the Boltzmann equation for the graviton distribution function at first order around a FLRW metric. We obtained the angular power spectrum of the SGWB, which includes the contributions from the initial anisotropy imprinted at the production of the GW and the one due to the propagation through the large-scale scalar and tensor perturbations of the universe.

In Chapter 3 in order to obtain the initial conditions for the GW energy density perturbation δ_{GW} and the evolution of gravitational potentials Φ and Ψ, we solved the Einstein equations combined with the Boltzmann equation for various particle species present in the universe at the time of the GW production. We considered adiabatic and isocurvature initial conditions and estimated the initial GW energy density perturbation δ_{GW} in each case.

In Chapter 4 the original results of the thesis are given. We studied whether the perturbations are adiabatic or isocurvature and affect the angular power spectrum of

SGWB. We presented the plots of the scale-invariant angular power spectrum of SGWB separately for adiabatic and isocurvature initial conditions, which we implemented numerically in the Boltzmann code CLASS, adapted for the SGWB. We found that on large scales the total power spectrum for CDM isocurvature perturbations is larger than the adiabatic one by the fraction $C_\ell^{iso}/C_\ell^{ad} \simeq 1.67$ due to the late ISW effect, which is important on large scales. The late ISW effect for the adiabatic perturbations is much larger than for the isocurvature one since the isocurvature primordial power spectrum is far smaller than the adiabatic one.

In the future, we plan to extend the analytic and numerical results obtained in this thesis to describe different primordial sources of GWs, in order to use the anisotropies as a tool to discriminate these mechanisms.

Bibliography

[1] B. P. Abbott et al. "Observation of Gravitational Waves from a Binary Black Hole Merger". In: *Phys. Rev. Lett.* 116.6 (2016), p. 061102. DOI: 10.1103/PhysRevLett.116.061102. arXiv: 1602.03837 [gr-qc].

[2] B. P. Abbott et al. "GW170817: Observation of Gravitational Waves from a Binary Neutron Star Inspiral". In: *Phys. Rev. Lett.* 119.16 (2017), p. 161101. DOI: 10.1103/PhysRevLett.119.161101. arXiv: 1710.05832 [gr-qc].

[3] Michele Maggiore et al. "Science Case for the Einstein Telescope". In: *JCAP* 03 (2020), p. 050. DOI: 10.1088/1475-7516/2020/03/050. arXiv: 1912.02622 [astro-ph.CO].

[4] Pau Amaro-Seoane et al. "Laser Interferometer Space Antenna". In: (Feb. 2017). arXiv: 1702.00786 [astro-ph.IM].

[5] T. J. W. Lazio. "The Square Kilometre Array pulsar timing array". In: *Class. Quant. Grav.* 30 (2013), p. 224011. DOI: 10.1088/0264-9381/30/22/224011.

[6] S. Kawamura et al. "The Japanese space gravitational wave antenna DECIGO". In: *Class. Quant. Grav.* 23 (2006). Ed. by N. Mio, S125–S132. DOI: 10.1088/0264-9381/23/8/S17.

[7] G. M. Harry, P. Fritschel, D. A. Shaddock, W. Folkner, and E. S. Phinney. "Laser interferometry for the big bang observer". In: *Class. Quant. Grav.* 23 (2006). [Erratum: Class.Quant.Grav. 23, 7361 (2006)], pp. 4887–4894. DOI: 10.1088/0264-9381/23/15/008.

[8] B. P. Abbott et al. "Search for the isotropic stochastic background using data from Advanced LIGO second observing run". In: *Phys. Rev. D* 100.6 (2019), p. 061101. DOI: 10.1103/PhysRevD.100.061101. arXiv: 1903.02886 [gr-qc].

[9] Nicola Bartolo et al. "Science with the space-based interferometer LISA. IV: Probing inflation with gravitational waves". In: *JCAP* 12 (2016), p. 026. DOI: 10.1088/1475-7516/2016/12/026. arXiv: 1610.06481 [astro-ph.CO].

[10] Chiara Caprini et al. "Science with the space-based interferometer eLISA. II: Gravitational waves from cosmological phase transitions". In: *JCAP* 04 (2016), p. 001. DOI: 10.1088/1475-7516/2016/04/001. arXiv: 1512.06239 [astro-ph.CO].

[11] Pierre Auclair et al. "Probing the gravitational wave background from cosmic strings with LISA". In: *JCAP* 04 (2020), p. 034. DOI: 10.1088/1475-7516/2020/04/034. arXiv: 1909.00819 [astro-ph.CO].

[12] Chiara Caprini, Daniel G. Figueroa, Raphael Flauger, Germano Nardini, Marco Peloso, Mauro Pieroni, Angelo Ricciardone, and Gianmassimo Tasinato. "Reconstructing the spectral shape of a stochastic gravitational wave background with LISA". In: *JCAP* 11 (2019), p. 017. DOI: 10.1088/1475-7516/2019/11/017. arXiv: 1906.09244 [astro-ph.CO].

[13] Vasyl Alba and Juan Maldacena. "Primordial gravity wave background anisotropies". In: *JHEP* 03 (2016), p. 115. DOI: 10.1007/JHEP03(2016)115. arXiv: 1512.01531 [hep-th].

[14] Carlo R. Contaldi. "Anisotropies of Gravitational Wave Backgrounds: A Line Of Sight Approach". In: *Phys. Lett. B* 771 (2017), pp. 9–12. DOI: 10.1016/j.physletb.2017.05.020. arXiv: 1609.08168 [astro-ph.CO].

[15] Alexander C. Jenkins and Mairi Sakellariadou. "Anisotropies in the stochastic gravitational-wave background: Formalism and the cosmic string case". In: *Phys. Rev. D* 98.6 (2018), p. 063509. DOI: 10.1103/PhysRevD.98.063509. arXiv: 1802.06046 [astro-ph.CO].

[16] Daniele Bertacca, Angelo Ricciardone, Nicola Bellomo, Alexander C. Jenkins, Sabino Matarrese, Alvise Raccanelli, Tania Regimbau, and Mairi Sakellariadou. "Projection effects on the observed angular spectrum of the astrophysical stochastic gravitational wave background". In: *Phys. Rev. D* 101.10 (2020), p. 103513. DOI: 10.1103/PhysRevD.101.103513. arXiv: 1909.11627 [astro-ph.CO].

[17] Neil Barnaby and Marco Peloso. "Large Nongaussianity in Axion Inflation". In: *Phys. Rev. Lett.* 106 (2011), p. 181301. DOI: 10.1103/PhysRevLett.106.181301. arXiv: 1011.1500 [hep-ph].

[18] N. Bartolo, S. Matarrese, A. Riotto, and A. Vaihkonen. "The Maximal Amount of Gravitational Waves in the Curvaton Scenario". In: *Phys. Rev. D* 76 (2007), p. 061302. DOI: 10.1103/PhysRevD.76.061302. arXiv: 0705.4240 [astro-ph].

[19] Rachel Jeannerot, Jonathan Rocher, and Mairi Sakellariadou. "How generic is cosmic string formation in SUSY GUTs". In: *Phys. Rev. D* 68 (2003), p. 103514. DOI: 10.1103/PhysRevD.68.103514. arXiv: hep-ph/0308134.

[20] Saswat Sarangi and S. H. Henry Tye. "Cosmic string production towards the end of brane inflation". In: *Phys. Lett. B* 536 (2002), pp. 185–192. DOI: 10.1016/S0370-2693(02)01824-5. arXiv: hep-th/0204074.

[21] Tanmay Vachaspati, Levon Pogosian, and Daniele Steer. "Cosmic Strings". In: *Scholarpedia* 10.2 (2015), p. 31682. DOI: 10.4249/scholarpedia.31682. arXiv: 1506.04039 [astro-ph.CO].

[22] N. Bartolo, D. Bertacca, S. Matarrese, M. Peloso, A. Ricciardone, A. Riotto, and G. Tasinato. "Anisotropies and non-Gaussianity of the Cosmological Gravitational Wave Background". In: *Phys. Rev. D* 100.12 (2019), p. 121501. DOI: 10.1103/PhysRevD.100.121501. arXiv: 1908.00527 [astro-ph.CO].

[23] Angelo Ricciardone, Lorenzo Valbusa Dall'Armi, Nicola Bartolo, Daniele Bertacca, Michele Liguori, and Sabino Matarrese. "Cross-Correlating Astrophysical and Cosmological Gravitational Wave Backgrounds with the Cosmic Microwave Background". In: *Phys. Rev. Lett.* 127.27 (2021), p. 271301. DOI: 10.1103/PhysRevLett.127.271301. arXiv: 2106.02591 [astro-ph.CO].

[24] L. Valbusa Dall'Armi, A. Ricciardone, Nicola Bartolo, D. Bertacca, and S. Matarrese. "Imprint of relativistic particles on the anisotropies of the stochastic gravitational-wave background". In: *Phys. Rev. D* 103.2 (2021), p. 023522. DOI: 10.1103/PhysRevD.103.023522. arXiv: 2007.01215 [astro-ph.CO].

[25] Nicola Bartolo, Daniele Bertacca, Sabino Matarrese, Marco Peloso, Angelo Ricciardone, Antonio Riotto, and Gianmassimo Tasinato. "Characterizing the cosmological gravitational wave background: Anisotropies and non-Gaussianity". In: *Phys. Rev. D* 102.2 (2020), p. 023527. DOI: 10.1103/PhysRevD.102.023527. arXiv: 1912.09433 [astro-ph.CO].

[26] Scott Dodelson. *Modern Cosmology*. Amsterdam: Academic Press, 2003. ISBN: 978-0-12-219141-1.

[27] P. P. Avelino and R. R. Caldwell. "Entropy perturbations due to cosmic strings". In: *Phys. Rev. D* 53 (1996), R5339–R5343. DOI: 10.1103/PhysRevD.53.R5339. arXiv: astro-ph/9602116.

[28] Soubhik Kumar, Raman Sundrum, and Yuhsin Tsai. "Non-Gaussian stochastic gravitational waves from phase transitions". In: *JHEP* 11 (2021), p. 107. DOI: 10.1007/JHEP11(2021)107. arXiv: 2102.05665 [astro-ph.CO].

[29] Julien Lesgourgues. "The Cosmic Linear Anisotropy Solving System (CLASS) I: Overview". In: (Apr. 2011). arXiv: 1104.2932 [astro-ph.IM].

[30] Alan H. Guth. "The Inflationary Universe: A Possible Solution to the Horizon and Flatness Problems". In: *Phys. Rev. D* 23 (1981). Ed. by Li-Zhi Fang and R. Ruffini, pp. 347–356. DOI: 10.1103/PhysRevD.23.347.

[31] Alan H. Guth and S. Y. Pi. "Fluctuations in the New Inflationary Universe". In: *Phys. Rev. Lett.* 49 (1982), pp. 1110–1113. DOI: 10.1103/PhysRevLett.49.1110.

[32] James M. Bardeen, Paul J. Steinhardt, and Michael S. Turner. "Spontaneous Creation of Almost Scale - Free Density Perturbations in an Inflationary Universe". In: *Phys. Rev. D* 28 (1983), p. 679. DOI: 10.1103/PhysRevD.28.679.

[33] Claus Kiefer, David Polarski, and Alexei A. Starobinsky. "Quantum to classical transition for fluctuations in the early universe". In: *Int. J. Mod. Phys. D* 7 (1998), pp. 455–462. DOI: 10.1142/S0218271898000292. arXiv: gr-qc/9802003.

[34] Chiara Caprini and Daniel G. Figueroa. "Cosmological Backgrounds of Gravitational Waves". In: *Class. Quant. Grav.* 35.16 (2018), p. 163001. DOI: 10.1088/1361-6382/aac608. arXiv: 1801.04268 [astro-ph.CO].

[35] Yuki Watanabe and Eiichiro Komatsu. "Improved Calculation of the Primordial Gravitational Wave Spectrum in the Standard Model". In: *Phys. Rev. D* 73 (2006), p. 123515. DOI: 10.1103/PhysRevD.73.123515. arXiv: astro-ph/0604176.

[36] P. A. R. Ade et al. "Planck 2015 results. XX. Constraints on inflation". In: *Astron. Astrophys.* 594 (2016), A20. DOI: 10.1051/0004-6361/201525898. arXiv: 1502.02114 [astro-ph.CO].

[37] Andrew R. Liddle and David H. Lyth. "COBE, gravitational waves, inflation and extended inflation". In: *Phys. Lett. B* 291 (1992), pp. 391–398. DOI: 10.1016/0370-2693(92)91393-N. arXiv: astro-ph/9208007.

[38] M. Tristram et al. "Improved limits on the tensor-to-scalar ratio using BICEP and Planck data". In: *Phys. Rev. D* 105.8 (2022), p. 083524. DOI: 10.1103/PhysRevD.105.083524. arXiv: 2112.07961 [astro-ph.CO].

[39] Eric Thrane and Joseph D. Romano. "Sensitivity curves for searches for gravitational-wave backgrounds". In: *Phys. Rev. D* 88.12 (2013), p. 124032. DOI: 10.1103/PhysRevD.88.124032. arXiv: 1310.5300 [astro-ph.IM].

[40] Kai Schmitz. "LISA Sensitivity to Gravitational Waves from Sound Waves". In: *Symmetry* 12.9 (2020), p. 1477. DOI: 10.3390/sym12091477. arXiv: 2005.10789 [hep-ph].

[41] Vincent Corbin and Neil J. Cornish. "Detecting the cosmic gravitational wave background with the big bang observer". In: *Class. Quant. Grav.* 23 (2006), pp. 2435–2446. DOI: 10.1088/0264-9381/23/7/014. arXiv: gr-qc/0512039.

[42] Seiji Kawamura et al. "The Japanese space gravitational wave antenna: DECIGO". In: *Class. Quant. Grav.* 28 (2011). Ed. by Sasha Buchman and Ke-Xun Sun, p. 094011. DOI: 10.1088/0264-9381/28/9/094011.

[43] Mohamed M. Anber and Lorenzo Sorbo. "N-flationary magnetic fields". In: *JCAP* 10 (2006), p. 018. DOI: 10.1088/1475-7516/2006/10/018. arXiv: astro-ph/0606534.

[44] P. A. R. Ade et al. "Planck 2015 results. XVII. Constraints on primordial non-Gaussianity". In: *Astron. Astrophys.* 594 (2016), A17. DOI: 10.1051/0004-6361/201525836. arXiv: 1502.01592 [astro-ph.CO].

[45] Lorenzo Sorbo. "Parity violation in the Cosmic Microwave Background from a pseudoscalar inflaton". In: *JCAP* 06 (2011), p. 003. DOI: 10.1088/1475-7516/2011/06/003. arXiv: 1101.1525 [astro-ph.CO].

[46] Tomohiro Fujita, Jun'ichi Yokoyama, and Shuichiro Yokoyama. "Can a spectator scalar field enhance inflationary tensor mode?" In: *PTEP* 2015 (2015), 043E01. DOI: 10.1093/ptep/ptv037. arXiv: 1411.3658 [astro-ph.CO].

[47] David H. Lyth and David Wands. "Generating the curvature perturbation without an inflaton". In: *Phys. Lett. B* 524 (2002), pp. 5–14. DOI: 10.1016/S0370-2693(01)01366-1. arXiv: hep-ph/0110002.

[48] David H. Lyth, Carlo Ungarelli, and David Wands. "The Primordial density perturbation in the curvaton scenario". In: *Phys. Rev. D* 67 (2003), p. 023503. DOI: 10.1103/PhysRevD.67.023503. arXiv: astro-ph/0208055.

[49] N. Bartolo, S. Matarrese, and A. Riotto. "On nonGaussianity in the curvaton scenario". In: *Phys. Rev. D* 69 (2004), p. 043503. DOI: 10.1103/PhysRevD.69.043503. arXiv: hep-ph/0309033.

[50] Y. Akrami et al. "Planck 2018 results. IX. Constraints on primordial non-Gaussianity". In: *Astron. Astrophys.* 641 (2020), A9. DOI: 10.1051/0004-6361/201935891. arXiv: 1905.05697 [astro-ph.CO].

[51] K. Kajantie, M. Laine, K. Rummukainen, and Mikhail E. Shaposhnikov. "Is there a hot electroweak phase transition at $m_H \geq m_W$?" In: *Phys. Rev. Lett.* 77 (1996), pp. 2887–2890. DOI: 10.1103/PhysRevLett.77.2887. arXiv: hep-ph/9605288.

[52] Chiara Caprini, Ruth Durrer, and Geraldine Servant. "Gravitational wave generation from bubble collisions in first-order phase transitions: An analytic approach". In: *Phys. Rev. D* 77 (2008), p. 124015. DOI: 10.1103/PhysRevD.77.124015. arXiv: 0711.2593 [astro-ph].

[53] Christophe Grojean and Geraldine Servant. "Gravitational Waves from Phase Transitions at the Electroweak Scale and Beyond". In: *Phys. Rev. D* 75 (2007), p. 043507. DOI: 10.1103/PhysRevD.75.043507. arXiv: hep-ph/0607107.

[54] Pierre Binetruy, Alejandro Bohe, Chiara Caprini, and Jean-Francois Dufaux. "Cosmological Backgrounds of Gravitational Waves and eLISA/NGO: Phase Transitions, Cosmic Strings and Other Sources". In: *JCAP* 06 (2012), p. 027. DOI: 10.1088/1475-7516/2012/06/027. arXiv: 1201.0983 [gr-qc].

[55] Arthur Kosowsky, Michael S. Turner, and Richard Watkins. "Gravitational radiation from colliding vacuum bubbles". In: *Phys. Rev. D* 45 (1992), pp. 4514–4535. DOI: 10.1103/PhysRevD.45.4514.

[56] Arthur Kosowsky and Michael S. Turner. "Gravitational radiation from colliding vacuum bubbles: envelope approximation to many bubble collisions". In: *Phys. Rev. D* 47 (1993), pp. 4372–4391. DOI: 10.1103/PhysRevD.47.4372. arXiv: astro-ph/9211004.

[57] Stephan J. Huber and Thomas Konstandin. "Gravitational Wave Production by Collisions: More Bubbles". In: *JCAP* 09 (2008), p. 022. DOI: 10.1088/1475-7516/2008/09/022. arXiv: 0806.1828 [hep-ph].

[58] Mark Hindmarsh, Stephan J. Huber, Kari Rummukainen, and David J. Weir. "Numerical simulations of acoustically generated gravitational waves at a first order phase transition". In: *Phys. Rev. D* 92.12 (2015), p. 123009. DOI: 10.1103/PhysRevD.92.123009. arXiv: 1504.03291 [astro-ph.CO].

[59] Arthur Kosowsky, Andrew Mack, and Tinatin Kahniashvili. "Gravitational radiation from cosmological turbulence". In: *Phys. Rev. D* 66 (2002), p. 024030. DOI: 10.1103/PhysRevD.66.024030. arXiv: astro-ph/0111483.

[60] Chiara Caprini, Ruth Durrer, and Geraldine Servant. "The stochastic gravitational wave background from turbulence and magnetic fields generated by a first-order phase transition". In: *JCAP* 12 (2009), p. 024. DOI: 10.1088/1475-7516/2009/12/024. arXiv: 0909.0622 [astro-ph.CO].

[61] Dietrich Bodeker and Guy D. Moore. "Can electroweak bubble walls run away?" In: *JCAP* 05 (2009), p. 009. DOI: 10.1088/1475-7516/2009/05/009. arXiv: 0903.4099 [hep-ph].

[62] Jose R. Espinosa, Thomas Konstandin, Jose M. No, and Geraldine Servant. "Energy Budget of Cosmological First-order Phase Transitions". In: *JCAP* 06 (2010), p. 028. DOI: 10.1088/1475-7516/2010/06/028. arXiv: 1004.4187 [hep-ph].

[63] Jose J. Blanco-Pillado, Ken D. Olum, and Benjamin Shlaer. "The number of cosmic string loops". In: *Phys. Rev. D* 89.2 (2014), p. 023512. DOI: 10.1103/PhysRevD.89.023512. arXiv: 1309.6637 [astro-ph.CO].

[64] J. Dunkley et al. "The Atacama Cosmology Telescope: Cosmological Parameters from the 2008 Power Spectra". In: *Astrophys. J.* 739 (2011), p. 52. DOI: 10.1088/0004-637X/739/1/52. arXiv: 1009.0866 [astro-ph.CO].

[65] Nicola Bartolo, Valerie Domcke, Daniel G. Figueroa, Juan Garcıa-Bellido, Marco Peloso, Mauro Pieroni, Angelo Ricciardone, Mairi Sakellariadou, Lorenzo Sorbo, and Gianmassimo Tasinato. "Probing non-Gaussian Stochastic Gravitational Wave Backgrounds with LISA". In: *JCAP* 11 (2018), p. 034. DOI: 10.1088/1475-7516/2018/11/034. arXiv: 1806.02819 [astro-ph.CO].

[66] Y. Akrami et al. "Planck 2018 results. X. Constraints on inflation". In: *Astron. Astrophys.* 641 (2020), A10. DOI: 10.1051/0004-6361/201833887. arXiv: 1807.06211 [astro-ph.CO].

[67] N. Aghanim et al. "Planck 2018 results. VI. Cosmological parameters". In: *Astron. Astrophys.* 641 (2020). [Erratum: Astron.Astrophys. 652, C4 (2021)], A6. DOI: 10.1051/0004-6361/201833910. arXiv: 1807.06209 [astro-ph.CO].

[68] Martin Bucher, Kavilan Moodley, and Neil Turok. "The General primordial cosmic perturbation". In: *Phys. Rev. D* 62 (2000), p. 083508. DOI: 10.1103/PhysRevD.62.083508. arXiv: astro-ph/9904231.

[69] Chung-Pei Ma and Edmund Bertschinger. "Cosmological perturbation theory in the synchronous and conformal Newtonian gauges". In: *Astrophys. J.* 455 (1995), pp. 7–25. DOI: 10.1086/176550. arXiv: astro-ph/9506072.

Bibliography

[1] B. P. Abbott et al. "Observation of Gravitational Waves from a Binary Black Hole Merger". In: *Phys. Rev. Lett.* 116.6 (2016), p. 061102. DOI: 10.1103/PhysRevLett.116.061102. arXiv: 1602.03837 [gr-qc].

[2] B. P. Abbott et al. "GW170817: Observation of Gravitational Waves from a Binary Neutron Star Inspiral". In: *Phys. Rev. Lett.* 119.16 (2017), p. 161101. DOI: 10.1103/PhysRevLett.119.161101. arXiv: 1710.05832 [gr-qc].

[3] Michele Maggiore et al. "Science Case for the Einstein Telescope". In: *JCAP* 03 (2020), p. 050. DOI: 10.1088/1475-7516/2020/03/050. arXiv: 1912.02622 [astro-ph.CO].

[4] Pau Amaro-Seoane et al. "Laser Interferometer Space Antenna". In: (Feb. 2017). arXiv: 1702.00786 [astro-ph.IM].

[5] T. J. W. Lazio. "The Square Kilometre Array pulsar timing array". In: *Class. Quant. Grav.* 30 (2013), p. 224011. DOI: 10.1088/0264-9381/30/22/224011.

[6] S. Kawamura et al. "The Japanese space gravitational wave antenna DECIGO". In: *Class. Quant. Grav.* 23 (2006). Ed. by N. Mio, S125–S132. DOI: 10.1088/0264-9381/23/8/S17.

[7] G. M. Harry, P. Fritschel, D. A. Shaddock, W. Folkner, and E. S. Phinney. "Laser interferometry for the big bang observer". In: *Class. Quant. Grav.* 23 (2006). [Erratum: Class.Quant.Grav. 23, 7361 (2006)], pp. 4887–4894. DOI: 10.1088/0264-9381/23/15/008.

[8] B. P. Abbott et al. "Search for the isotropic stochastic background using data from Advanced LIGO second observing run". In: *Phys. Rev. D* 100.6 (2019), p. 061101. DOI: 10.1103/PhysRevD.100.061101. arXiv: 1903.02886 [gr-qc].

[9] Nicola Bartolo et al. "Science with the space-based interferometer LISA. IV: Probing inflation with gravitational waves". In: *JCAP* 12 (2016), p. 026. DOI: 10.1088/1475-7516/2016/12/026. arXiv: 1610.06481 [astro-ph.CO].

[10] Chiara Caprini et al. "Science with the space-based interferometer eLISA. II: Gravitational waves from cosmological phase transitions". In: *JCAP* 04 (2016), p. 001. DOI: 10.1088/1475-7516/2016/04/001. arXiv: 1512.06239 [astro-ph.CO].

[11] Pierre Auclair et al. "Probing the gravitational wave background from cosmic strings with LISA". In: *JCAP* 04 (2020), p. 034. DOI: 10.1088/1475-7516/2020/04/034. arXiv: 1909.00819 [astro-ph.CO].

[12] Chiara Caprini, Daniel G. Figueroa, Raphael Flauger, Germano Nardini, Marco Peloso, Mauro Pieroni, Angelo Ricciardone, and Gianmassimo Tasinato. "Reconstructing the spectral shape of a stochastic gravitational wave background with LISA". In: *JCAP* 11 (2019), p. 017. DOI: 10.1088/1475-7516/2019/11/017. arXiv: 1906.09244 [astro-ph.CO].

[13] Vasyl Alba and Juan Maldacena. "Primordial gravity wave background anisotropies". In: *JHEP* 03 (2016), p. 115. DOI: 10.1007/JHEP03(2016)115. arXiv: 1512.01531 [hep-th].

[14] Carlo R. Contaldi. "Anisotropies of Gravitational Wave Backgrounds: A Line Of Sight Approach". In: *Phys. Lett. B* 771 (2017), pp. 9–12. DOI: 10.1016/j.physletb.2017.05.020. arXiv: 1609.08168 [astro-ph.CO].

[15] Alexander C. Jenkins and Mairi Sakellariadou. "Anisotropies in the stochastic gravitational-wave background: Formalism and the cosmic string case". In: *Phys. Rev. D* 98.6 (2018), p. 063509. DOI: 10.1103/PhysRevD.98.063509. arXiv: 1802.06046 [astro-ph.CO].

[16] Daniele Bertacca, Angelo Ricciardone, Nicola Bellomo, Alexander C. Jenkins, Sabino Matarrese, Alvise Raccanelli, Tania Regimbau, and Mairi Sakellariadou. "Projection effects on the observed angular spectrum of the astrophysical stochastic gravitational wave background". In: *Phys. Rev. D* 101.10 (2020), p. 103513. DOI: 10.1103/PhysRevD.101.103513. arXiv: 1909.11627 [astro-ph.CO].

[17] Neil Barnaby and Marco Peloso. "Large Nongaussianity in Axion Inflation". In: *Phys. Rev. Lett.* 106 (2011), p. 181301. DOI: 10.1103/PhysRevLett.106.181301. arXiv: 1011.1500 [hep-ph].

[18] N. Bartolo, S. Matarrese, A. Riotto, and A. Vaihkonen. "The Maximal Amount of Gravitational Waves in the Curvaton Scenario". In: *Phys. Rev. D* 76 (2007), p. 061302. DOI: 10.1103/PhysRevD.76.061302. arXiv: 0705.4240 [astro-ph].

[19] Rachel Jeannerot, Jonathan Rocher, and Mairi Sakellariadou. "How generic is cosmic string formation in SUSY GUTs". In: *Phys. Rev. D* 68 (2003), p. 103514. DOI: 10.1103/PhysRevD.68.103514. arXiv: hep-ph/0308134.

[20] Saswat Sarangi and S. H. Henry Tye. "Cosmic string production towards the end of brane inflation". In: *Phys. Lett. B* 536 (2002), pp. 185–192. DOI: 10.1016/S0370-2693(02)01824-5. arXiv: hep-th/0204074.

[21] Tanmay Vachaspati, Levon Pogosian, and Daniele Steer. "Cosmic Strings". In: *Scholarpedia* 10.2 (2015), p. 31682. DOI: 10.4249/scholarpedia.31682. arXiv: 1506.04039 [astro-ph.CO].

[22] N. Bartolo, D. Bertacca, S. Matarrese, M. Peloso, A. Ricciardone, A. Riotto, and G. Tasinato. "Anisotropies and non-Gaussianity of the Cosmological Gravitational Wave Background". In: *Phys. Rev. D* 100.12 (2019), p. 121501. DOI: 10.1103/PhysRevD.100.121501. arXiv: 1908.00527 [astro-ph.CO].

[23] Angelo Ricciardone, Lorenzo Valbusa Dall'Armi, Nicola Bartolo, Daniele Bertacca, Michele Liguori, and Sabino Matarrese. "Cross-Correlating Astrophysical and Cosmological Gravitational Wave Backgrounds with the Cosmic Microwave Background". In: *Phys. Rev. Lett.* 127.27 (2021), p. 271301. DOI: 10.1103/PhysRevLett.127.271301. arXiv: 2106.02591 [astro-ph.CO].

[24] L. Valbusa Dall'Armi, A. Ricciardone, Nicola Bartolo, D. Bertacca, and S. Matarrese. "Imprint of relativistic particles on the anisotropies of the stochastic gravitational-wave background". In: *Phys. Rev. D* 103.2 (2021), p. 023522. DOI: 10.1103/PhysRevD.103.023522. arXiv: 2007.01215 [astro-ph.CO].

[25] Nicola Bartolo, Daniele Bertacca, Sabino Matarrese, Marco Peloso, Angelo Ricciardone, Antonio Riotto, and Gianmassimo Tasinato. "Characterizing the cosmological gravitational wave background: Anisotropies and non-Gaussianity". In: *Phys. Rev. D* 102.2 (2020), p. 023527. DOI: 10.1103/PhysRevD.102.023527. arXiv: 1912.09433 [astro-ph.CO].

[26] Scott Dodelson. *Modern Cosmology*. Amsterdam: Academic Press, 2003. ISBN: 978-0-12-219141-1.

[27] P. P. Avelino and R. R. Caldwell. "Entropy perturbations due to cosmic strings". In: *Phys. Rev. D* 53 (1996), R5339–R5343. DOI: 10.1103/PhysRevD.53.R5339. arXiv: astro-ph/9602116.

[28] Soubhik Kumar, Raman Sundrum, and Yuhsin Tsai. "Non-Gaussian stochastic gravitational waves from phase transitions". In: *JHEP* 11 (2021), p. 107. DOI: 10.1007/JHEP11(2021)107. arXiv: 2102.05665 [astro-ph.CO].

[29] Julien Lesgourgues. "The Cosmic Linear Anisotropy Solving System (CLASS) I: Overview". In: (Apr. 2011). arXiv: 1104.2932 [astro-ph.IM].

[30] Alan H. Guth. "The Inflationary Universe: A Possible Solution to the Horizon and Flatness Problems". In: *Phys. Rev. D* 23 (1981). Ed. by Li-Zhi Fang and R. Ruffini, pp. 347–356. DOI: 10.1103/PhysRevD.23.347.

[31] Alan H. Guth and S. Y. Pi. "Fluctuations in the New Inflationary Universe". In: *Phys. Rev. Lett.* 49 (1982), pp. 1110–1113. DOI: 10.1103/PhysRevLett.49.1110.

[32] James M. Bardeen, Paul J. Steinhardt, and Michael S. Turner. "Spontaneous Creation of Almost Scale - Free Density Perturbations in an Inflationary Universe". In: *Phys. Rev. D* 28 (1983), p. 679. DOI: 10.1103/PhysRevD.28.679.

[33] Claus Kiefer, David Polarski, and Alexei A. Starobinsky. "Quantum to classical transition for fluctuations in the early universe". In: *Int. J. Mod. Phys. D* 7 (1998), pp. 455–462. DOI: 10.1142/S0218271898000292. arXiv: gr-qc/9802003.

[34] Chiara Caprini and Daniel G. Figueroa. "Cosmological Backgrounds of Gravitational Waves". In: *Class. Quant. Grav.* 35.16 (2018), p. 163001. DOI: 10.1088/1361-6382/aac608. arXiv: 1801.04268 [astro-ph.CO].

[35] Yuki Watanabe and Eiichiro Komatsu. "Improved Calculation of the Primordial Gravitational Wave Spectrum in the Standard Model". In: *Phys. Rev. D* 73 (2006), p. 123515. DOI: 10.1103/PhysRevD.73.123515. arXiv: astro-ph/0604176.

[36] P. A. R. Ade et al. "Planck 2015 results. XX. Constraints on inflation". In: *Astron. Astrophys.* 594 (2016), A20. DOI: 10.1051/0004-6361/201525898. arXiv: 1502.02114 [astro-ph.CO].

[37] Andrew R. Liddle and David H. Lyth. "COBE, gravitational waves, inflation and extended inflation". In: *Phys. Lett. B* 291 (1992), pp. 391–398. DOI: 10.1016/0370-2693(92)91393-N. arXiv: astro-ph/9208007.

[38] M. Tristram et al. "Improved limits on the tensor-to-scalar ratio using BICEP and Planck data". In: *Phys. Rev. D* 105.8 (2022), p. 083524. DOI: 10.1103/PhysRevD.105.083524. arXiv: 2112.07961 [astro-ph.CO].

[39] Eric Thrane and Joseph D. Romano. "Sensitivity curves for searches for gravitational-wave backgrounds". In: *Phys. Rev. D* 88.12 (2013), p. 124032. DOI: 10.1103/PhysRevD.88.124032. arXiv: 1310.5300 [astro-ph.IM].

[40] Kai Schmitz. "LISA Sensitivity to Gravitational Waves from Sound Waves". In: *Symmetry* 12.9 (2020), p. 1477. DOI: 10.3390/sym12091477. arXiv: 2005.10789 [hep-ph].

[41] Vincent Corbin and Neil J. Cornish. "Detecting the cosmic gravitational wave background with the big bang observer". In: *Class. Quant. Grav.* 23 (2006), pp. 2435–2446. DOI: 10.1088/0264-9381/23/7/014. arXiv: gr-qc/0512039.

[42] Seiji Kawamura et al. "The Japanese space gravitational wave antenna: DECIGO". In: *Class. Quant. Grav.* 28 (2011). Ed. by Sasha Buchman and Ke-Xun Sun, p. 094011. DOI: 10.1088/0264-9381/28/9/094011.

[43] Mohamed M. Anber and Lorenzo Sorbo. "N-flationary magnetic fields". In: *JCAP* 10 (2006), p. 018. DOI: 10.1088/1475-7516/2006/10/018. arXiv: astro-ph/0606534.

[44] P. A. R. Ade et al. "Planck 2015 results. XVII. Constraints on primordial non-Gaussianity". In: *Astron. Astrophys.* 594 (2016), A17. DOI: 10.1051/0004-6361/201525836. arXiv: 1502.01592 [astro-ph.CO].

[45] Lorenzo Sorbo. "Parity violation in the Cosmic Microwave Background from a pseudoscalar inflaton". In: *JCAP* 06 (2011), p. 003. DOI: 10.1088/1475-7516/2011/06/003. arXiv: 1101.1525 [astro-ph.CO].

[46] Tomohiro Fujita, Jun'ichi Yokoyama, and Shuichiro Yokoyama. "Can a spectator scalar field enhance inflationary tensor mode?" In: *PTEP* 2015 (2015), 043E01. DOI: 10.1093/ptep/ptv037. arXiv: 1411.3658 [astro-ph.CO].

[47] David H. Lyth and David Wands. "Generating the curvature perturbation without an inflaton". In: *Phys. Lett. B* 524 (2002), pp. 5–14. DOI: 10.1016/S0370-2693(01)01366-1. arXiv: hep-ph/0110002.

[48] David H. Lyth, Carlo Ungarelli, and David Wands. "The Primordial density perturbation in the curvaton scenario". In: *Phys. Rev. D* 67 (2003), p. 023503. DOI: 10.1103/PhysRevD.67.023503. arXiv: astro-ph/0208055.

[49] N. Bartolo, S. Matarrese, and A. Riotto. "On nonGaussianity in the curvaton scenario". In: *Phys. Rev. D* 69 (2004), p. 043503. DOI: 10.1103/PhysRevD.69.043503. arXiv: hep-ph/0309033.

[50] Y. Akrami et al. "Planck 2018 results. IX. Constraints on primordial non-Gaussianity". In: *Astron. Astrophys.* 641 (2020), A9. DOI: 10.1051/0004-6361/201935891. arXiv: 1905.05697 [astro-ph.CO].

[51] K. Kajantie, M. Laine, K. Rummukainen, and Mikhail E. Shaposhnikov. "Is there a hot electroweak phase transition at $m_H \geq m_W$?" In: *Phys. Rev. Lett.* 77 (1996), pp. 2887–2890. DOI: 10.1103/PhysRevLett.77.2887. arXiv: hep-ph/9605288.

[52] Chiara Caprini, Ruth Durrer, and Geraldine Servant. "Gravitational wave generation from bubble collisions in first-order phase transitions: An analytic approach". In: *Phys. Rev. D* 77 (2008), p. 124015. DOI: 10.1103/PhysRevD.77.124015. arXiv: 0711.2593 [astro-ph].

[53] Christophe Grojean and Geraldine Servant. "Gravitational Waves from Phase Transitions at the Electroweak Scale and Beyond". In: *Phys. Rev. D* 75 (2007), p. 043507. DOI: 10.1103/PhysRevD.75.043507. arXiv: hep-ph/0607107.

[54] Pierre Binetruy, Alejandro Bohe, Chiara Caprini, and Jean-Francois Dufaux. "Cosmological Backgrounds of Gravitational Waves and eLISA/NGO: Phase Transitions, Cosmic Strings and Other Sources". In: *JCAP* 06 (2012), p. 027. DOI: 10.1088/1475-7516/2012/06/027. arXiv: 1201.0983 [gr-qc].

[55] Arthur Kosowsky, Michael S. Turner, and Richard Watkins. "Gravitational radiation from colliding vacuum bubbles". In: *Phys. Rev. D* 45 (1992), pp. 4514–4535. DOI: 10.1103/PhysRevD.45.4514.

[56] Arthur Kosowsky and Michael S. Turner. "Gravitational radiation from colliding vacuum bubbles: envelope approximation to many bubble collisions". In: *Phys. Rev. D* 47 (1993), pp. 4372–4391. DOI: 10.1103/PhysRevD.47.4372. arXiv: astro-ph/9211004.

[57] Stephan J. Huber and Thomas Konstandin. "Gravitational Wave Production by Collisions: More Bubbles". In: *JCAP* 09 (2008), p. 022. DOI: 10.1088/1475-7516/2008/09/022. arXiv: 0806.1828 [hep-ph].

[58] Mark Hindmarsh, Stephan J. Huber, Kari Rummukainen, and David J. Weir. "Numerical simulations of acoustically generated gravitational waves at a first order phase transition". In: *Phys. Rev. D* 92.12 (2015), p. 123009. DOI: 10.1103/PhysRevD.92.123009. arXiv: 1504.03291 [astro-ph.CO].

[59] Arthur Kosowsky, Andrew Mack, and Tinatin Kahniashvili. "Gravitational radiation from cosmological turbulence". In: *Phys. Rev. D* 66 (2002), p. 024030. DOI: 10.1103/PhysRevD.66.024030. arXiv: astro-ph/0111483.

[60] Chiara Caprini, Ruth Durrer, and Geraldine Servant. "The stochastic gravitational wave background from turbulence and magnetic fields generated by a first-order phase transition". In: *JCAP* 12 (2009), p. 024. DOI: 10.1088/1475-7516/2009/12/024. arXiv: 0909.0622 [astro-ph.CO].

[61] Dietrich Bodeker and Guy D. Moore. "Can electroweak bubble walls run away?" In: *JCAP* 05 (2009), p. 009. DOI: 10.1088/1475-7516/2009/05/009. arXiv: 0903.4099 [hep-ph].

[62] Jose R. Espinosa, Thomas Konstandin, Jose M. No, and Geraldine Servant. "Energy Budget of Cosmological First-order Phase Transitions". In: *JCAP* 06 (2010), p. 028. DOI: 10.1088/1475-7516/2010/06/028. arXiv: 1004.4187 [hep-ph].

[63] Jose J. Blanco-Pillado, Ken D. Olum, and Benjamin Shlaer. "The number of cosmic string loops". In: *Phys. Rev. D* 89.2 (2014), p. 023512. DOI: 10.1103/PhysRevD.89.023512. arXiv: 1309.6637 [astro-ph.CO].

[64] J. Dunkley et al. "The Atacama Cosmology Telescope: Cosmological Parameters from the 2008 Power Spectra". In: *Astrophys. J.* 739 (2011), p. 52. DOI: 10.1088/0004-637X/739/1/52. arXiv: 1009.0866 [astro-ph.CO].

[65] Nicola Bartolo, Valerie Domcke, Daniel G. Figueroa, Juan Garcıa-Bellido, Marco Peloso, Mauro Pieroni, Angelo Ricciardone, Mairi Sakellariadou, Lorenzo Sorbo, and Gianmassimo Tasinato. "Probing non-Gaussian Stochastic Gravitational Wave Backgrounds with LISA". In: *JCAP* 11 (2018), p. 034. DOI: 10.1088/1475-7516/2018/11/034. arXiv: 1806.02819 [astro-ph.CO].

[66] Y. Akrami et al. "Planck 2018 results. X. Constraints on inflation". In: *Astron. Astrophys.* 641 (2020), A10. DOI: 10.1051/0004-6361/201833887. arXiv: 1807.06211 [astro-ph.CO].

[67] N. Aghanim et al. "Planck 2018 results. VI. Cosmological parameters". In: *Astron. Astrophys.* 641 (2020). [Erratum: Astron.Astrophys. 652, C4 (2021)], A6. DOI: 10.1051/0004-6361/201833910. arXiv: 1807.06209 [astro-ph.CO].

[68] Martin Bucher, Kavilan Moodley, and Neil Turok. "The General primordial cosmic perturbation". In: *Phys. Rev. D* 62 (2000), p. 083508. DOI: 10.1103/PhysRevD.62.083508. arXiv: astro-ph/9904231.

[69] Chung-Pei Ma and Edmund Bertschinger. "Cosmological perturbation theory in the synchronous and conformal Newtonian gauges". In: *Astrophys. J.* 455 (1995), pp. 7–25. DOI: 10.1086/176550. arXiv: astro-ph/9506072.